C1

Real-time monitoring of sinus node modulation in human infants: heart rate characteristics analysis in the diagnosis of neonatal sepsis

R. Moorman, P. Griffin and D. Lake

University of Virginia, Charlottesville, VA, USA

During sepsis, many organs fail. In a sense, sinus node failure is the loss of the fine adaptation of heart rate to external circumstance, and, indeed, loss of normal heart rate variability is a well-known feature of many human illnesses. In early development, sinus node failure is manifest as what we have called abnormal *heart rate characteristics* (HRC) of reduced variability and transient decelerations, and we found that these appear early in the course of neonatal sepsis and systemic inflammatory response syndrome. Inspection of the electrocardiograms confirms that all of the cardiac rhythm is sinus, affirming the link of the clinical findings to modulation of the sinus node. Since no conventional heart rate variability measure detects reduced variability and transient decelerations, we devised optimized measures for this purpose. These include sample asymmetry, a measure of heart rate histogram shape, and sample entropy, which is similar to the familiar approximate entropy but has better statistical properties and less bias. We developed a predictive statistical model that we call the *HRC index* that is highly associated with impending neonatal sepsis.

In clinical and mathematical studies, we have found that this HRC index is very highly significantly associated with imminent neonatal sepsis and death, rises before clinical signs of illness or abnormal laboratory test results, and is associated with neurodevelopmental outcome. In several neonatal intensive care units, monitored infants with neonatal sepsis have been diagnosed by positive blood cultures and treated with antibiotics without ever having signs of clinical illness.

New work has focused on the hypothesis that vagal discharge is the mechanism of the decelerations. Surprisingly, we find that during the transient heart rate decelerations, the AV conduction time, measured as the PR interval, decreases. We conclude that mechanism of transient heart rate decelerations is not necessarily due to vagal activation. Instead, we hypothesize that the mechanism includes abnormal sinus node intracellular signal transduction resulting in abnormal modulation of phase 4 depolarization. We further hypothesize that abnormal profiles of circulating cytokines are responsible.

Thus a measure of heart rate characteristics of reduced variability and transient decelerations is an early indicator of impending acute, severe neonatal illness. This clinical application of basic ideas about sinus node function and modulation may have benefit in clinical care of our most vulnerable patients.

Griffin MP, Lake DE, O'Shea TM, Moorman JR (2007). Pediatric Research 61, 222-227.

Griffin MP, Lake DE, Bissonette EA, Harrell FE, O'Shea TM, Moorman JR (2005). Pediatrics 116, 1070-1074.

Griffin MP, Lake DE, Moorman JR (2005). Pediatrics 115, 937-941.

Griffin MP, O'Shea TM, Bissonette EA, Harrell FE, Lake DE, Moorman JR (2003). Pediatric Research 53, 920-926.

Griffin MP, Moorman JR (2001). Pediatrics 107, 97-104.

Richman JS, Moorman JR (2000). American Journal of Physiology 278, H2039-2049.

Where applicable, the authors confirm that the experiments described here conform with The Physiological Society ethical requirements.

C2

Characterization and modulation of Tbx3 over-expressing mice

A. Engel[1], A.O. Verkerk[1], W.M. Hoogaars[2], V.M. Christoffels[2], E.E. Verheijck[1] and J.H. Ravesloot[1]

[1]Physiology, Academic Medical Center, Amsterdam, Netherlands and [2]Anatomy and Embryology, Academic Medical Center, Amsterdam, Netherlands

The T-box factor Tbx3 is important in the development of the sinoatrial node (SAN) by repressing the development from embryonic (nodal) primary myocardium to working myocardium.[1] When Tbx3 is artificially over-expressed in mouse atria from prenatal stages onwards, ectopic pacemaker regions are formed in the adult atria *in vivo*.[2] In this study, we characterized: 1) ECG parameters of such Tbx3 over-expressing mice, 2) whether Tbx3 over-expressing induced ectopic activity can be modulated by the chronotropic agents acetylcholine (ACh), and noradrenalin (NA), and 3) electrophysiological properties of single cells.

6-lead ECGs were recorded in isoflurane (~1.0%) anesthetized control mice and atrial Tbx3 over-expressing mice. Tbx3 over-expression atrial preparations devoid of SAN tissue and SAN preparations (with attached atria) of control mice were exposed to increasing NA (0.1-50 μM) or ACh (0.03-50 μM) concentrations. Sharp microelectrode impalements were used to analyse beating frequency. Finally, single cells were isolated by enzymatic dissociation.[3] Basic electrophysiological properties of Tbx3 over-expressing atrial and control SAN cells were assessed using perforated patch-clamp technique.

Tbx3 over-expressing mice revealed severe morphological changes in ECG characteristics, including short PQ intervals, double deflections in the P-wave and partially or complete atrioventricular-block, coinciding with shortened interbeat intervals. However, the average interbeat interval was comparable to those of control mice. Tbx3 over-expressing right atria were visibly hypertrophied. Intrinsic firing frequency was not significantly lower in Tbx3 over-expressing atria (4.1±0.6 (average±SEM, n=16) vs 5.2±0.4 Hz (control SAN; n=13)). ACh slowed, and NA accelerated spontaneous activity in a dose-dependent fashion in both Tbx3 over-expressing and control mice. Dose-frequency relationships of both ACh and NA in Tbx3 over-expressing and control mice were identical. 50% of the Tbx3 over-expressing atrial single cells showed spontaneous activity. Compared to control SAN cells (n=7), intrinsic firing frequency (5.2±0.9 (Tbx3) vs 6.5±0.7 Hz (control SAN)), and all other action potential parameters of Tbx3 over-expressing atrial cells (n=7) were not significantly different. The spontaneously active Tbx3 over-expressing atrial cells showed a hyperpolarization activated current, I_f, whose density was similar to that in control SAN cells. In the silent Tbx3 over-expressing atrial cells, I_f was virtually absent.

Embryonic Tbx3 over-expressing atria have electrophysiological features of SAN cells.

Hoogaars WMH et al. (2004). Cardiovasc. Res. 62, 489-499.

Hoogaars WMH et al. (2007). Genes & Dev. 21, 1098-1112.

Verheijck EE et al. (1995). Circ. Res. 76, 607-615.

Where applicable, the authors confirm that the experiments described here conform with The Physiological Society ethical requirements.

C3

Identification of residues involved in binding of ivabradine to hHCN4 channels

A. Bucchi, F. Rusconi, A. Splitt, A. Barbuti, M. Baruscotti and D. DiFrancesco

Università di Milano, Milano, Italy

Ivabradine is a molecule that selectively blocks the sinoatrial pacemaker "f" channels acting specifically from the intracellular site (1), and exclusively decreases heart rate without undesired cardiovascular side effects. Specifically, ivabradine has no negative inotropic or lusitropic effects and preserves ventricular contractility, and is therefore a primary tool in the pharmacological treatment of chronic stable angina (2).

Native f-channels are composed of HCN subunits, of which 4 isoforms are known. Experimental evidence indicates that f-channels are tetramers composed mostly of HCN4 subunits with a possible minor contribution of HCN1. The mechanisms of ivabradine block of sinoatrial f channels and HCN4 and HCN1 isoforms have been investigated in our laboratory (3,4). The properties of native and HCN4 channels block are similar, in that both display use- and current-dependence. The block of ivabradine of HCN1 channels, on the other hand, is still use-dependent but the current flow does not affect drug-channel interaction.

Data presented in this poster were collected with the aim of identifying critical residues in the pore-lining region involved in binding of ivabradine to human HCN4 channels. We focused our attention to two aminoacids (Y506 and I510) that are homologous to those involved in the binding of another I_f inhibitor compound (ZD7288) to HCN1 channel(5). We proceeded by individually substituting the two aminoacids by alanine residues (Y506A and I510A) and transfecting the mutated hHCN4 cDNAs into HEK293 cells. Electrophysiological studies were then performed in the whole-cell configuration at 32°C. We initially characterized the block with 30 μM drug by applying an activation/deactivation protocol (-140/+5 mV, 0.5 Hz) from a holding potential of -35 mV. Mean % blocks ± sem were 87.1±3.2 (n=5), 31.9±2.5 (n=4), and 41.2±6.0 (n=4) for wt, Y506A, and I510A channels, respectively. Statistical comparison revealed a decreased drug affinity for both mutations relative to wt channels ($p<0.05$, t-test). A full dose response was obtained for wt and Y506A channels; fitting with the Hill relation yielded Kd values of 1.6 μM and 56.1 μM and Hill slopes of 0.72 and 1.2, respectively; the two curves were significantly different ($p<0.001$, ANOVA).

Mean time constants of block onset ± sem induced by 30 μM ivabradine were 16.3±1.8 s (n=5), 26.9±11.6 s (n=4), and 12.0±3.0 s (n=4) for wt, Y506A, and I510A, respectively; no statistical differences were found ($p>0.05$, t-test), suggesting that the access of the drug to its binding site is not affected by the mutations. In conclusion, these data allow a preliminary identification of residues of the HCN4 channel that likely contribute to the binding of ivabradine and channel block.

Bois P, Bescond J, Renaudon B, Lenfant J (1996). Br J Pharmacol 118, 1051-7.

European Public Assessment Report (EPAR). Procoralan (2005): available at www.emea.eu.int

Bucchi A, Baruscotti M, DiFrancesco D (2002). J Gen Physiol 120, 1-13.

Bucchi A, Tognati A, Milanesi R, Baruscotti M, DiFrancesco D (2006). J Physiol 572, 335-46.

Shin KS, Rothberg BS, Yellen G (2001). J Gen Physiol 117, 91-101.

Supported by Servier International.

Where applicable, the authors confirm that the experiments described here conform with The Physiological Society ethical requirements.

C4

Optical mapping of human atrioventricular conduction

W.J. Hucker[1], V.V. Fedorov[1], K.V. Foyil[1], N. Moazami[2] and I.R. Efimov[1]

[1]Biomedical Engineering, Washington University in St. Louis, St. Louis, MO, USA and [2]Surgery, Washington University School of Medicine, St. Louis, MO, USA

The structure and function of the atrioventricular junction (AVJ) has been extensively studied for a century in many species. Historically, studies of the human AVJ were limited to postmortem histologic investigations because functional studies were not possible. With the advent of catheter based approaches, the function of the human AVJ has been studied and catheter based treatments have been developed. However catheter based approaches are limited both in the number of recording sites and the interventions possible to investigate AV conduction. In animal studies, optical mapping has emerged as the best technique to record electrophysiologic properties of nodal tissues, however this technique has not yet been applied to human AV conduction. In this study, we present the first instance of optical mapping of atrioventricular conduction in the human.

Explanted human hearts were obtained at the time of cardiac transplant from the transplant team at Washington University. The heart was removed from the body, perfused with cardioplegia, and transported to the laboratory. The AV nodal artery was cannulated and optical mapping was performed with a 16x16 photodiode array and the voltage sensitive dye Di-4-ANEPPS, in the presence of the excitation-contraction uncoupler blebbistatin (5uM) [1].

Optical action potentials (OAPs) were recorded from the interatrial septum, His bundle, AV node, slow pathway, and ventricular septum of human triangle of Koch preparations (n=2). S1S2 protocols repeatedly induced slow-fast reentrant beats: the slow pathway conducted anterogradely, followed by retrograde excitation of the fast pathway and subsequent excitation of the slow pathway again. When the slow pathway conducted to the His, the His electrogram had a different morphology than when the

fast pathway was responsible for His excitation, a phenomenon which indicates differential excitation of the His by the fast and slow pathways [2]. Additionally, a junctional rhythm was recorded from the His bundle region which demonstrated diastolic depolarization in the His OAP. The preparations that were functionally characterized will be studied with histology and immunohistochemistry to determine the precise structures and molecular characteristics responsible for OAPs.

This study is the first demonstration of optical mapping of conduction in the human AVJ during pacing, spontaneous activation, and AV nodal reentry. Our preliminary results reveal a pathway of AV nodal reentry, and our results indicate that optical mapping can be implemented to investigate the characteristics and mechanisms of human AV conduction in vitro.

Fedorov VV, Lozinsky IT, Sosunov EA, Anyukhovsky EP, Rosen MR, Balke CW, Efimov IR (2007). Heart Rhythm 4, 619-626.

Hucker WJ, Sharma V, Nikolski VP, Efimov IR (2007). Am J Physiol Heart Circ Physiol 0: 00115.2007v1.

Supported by American Heart Association and Stanley and Lucy Lopata Endowment.

Where applicable, the authors confirm that the experiments described here conform with The Physiological Society ethical requirements.

PC1

Cytosolic and nuclear calcium dynamics interaction in a three-dimensional ventricular E-Cell (3Dv E-Cell)

P. Li and A.V. Holden

Institute of Membrane and Systems Biology, University of Leeds, Leeds, UK

Earlier simulation studies have modelled the nucleus as a region lacking a releasable calcium pool with lower diffusion coefficient (about 50 $\mu m^2/s$) compared with cytoplasm (about 300 $\mu m^2/s$), where nuclear calcium rises only because of passive diffusion [1]. However, the magnitude and duration of nuclear calcium transient can be both significantly greater than that of cytosolic calcium transient, which indicates other potential nuclear calcium release sources [2].

Given the importance of nuclear calcium in the regulation gene transcription and expression, we introduce a nulcear envelope into the 3Dv E-Cell, which has been used to model stochastic intracellular calcium wave phenomena of an isolated ventricular cell [3], as a barrier with low diffusion coefficient $D_{NE} < 5$ $\mu m^2/s$ to maintain spatial heterogeneity, and nuclear calcium handling as a CICR type process with longer Ca^{2+} release duration (about 200 ms) and relative high diffusion coefficient (about 200 $\mu m^2/s$).

A nuclear envelope with a very low diffusion coefficient (D_{NE} = 0.1 $\mu m^2/s$), isolates the nucleus from the cytosol, and cytosolic calcium waves neither enter the nucleus nor initiate nuclear calcium transients. The nucleus acts simply as an obstacle that splits the calcium wave front into two fronts that travel around the nucleus.

For intermediate values (D_{NE} = 1.0 $\mu m^2/s$) a Ca^{2+} wave can trigger a confined nuclear Ca^{2+} transient, and lead to a nuclear Ca^{2+} excitation. Since the nucleus has a much longer Ca^{2+} release duration, nuclear Ca^{2+} concentration remains at a high level for a relatively long period after the cytosolic Ca^{2+} wave passed. At higher values (D_{NE} = 5.0 $\mu m^2/s$) a nuclear calcium transient can be activated when cytosolic calcium wave reached an end of the elongated nucleus. The nuclear Ca^{2+} transient can re-invade neighbouring cytosol and trigger a Ca^{2+} wave. This can allow a Ca^{2+} spark located near the nucleus to be amplified by the nuclear transient and nuclear envelope, and initiate a spontaneous cytosolic Ca^{2+} wave due to a high D_{NE}. Examples of these phenomena are illustrated in Fig. 1.

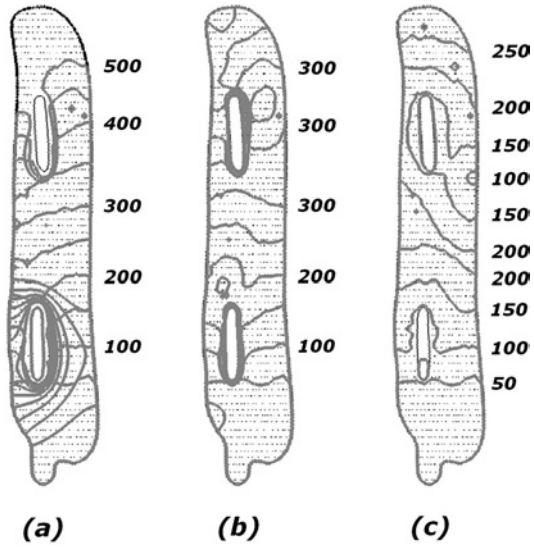

Fig. 1 Effects of the nuclear envelope diffusion coefficient on nuclear-cytosolic calcium transient coupling on intracellular calcium wave patterns. Isochrones of 20μM [Ca^{2+}] are shown with time steps of 50ms. At t = 0ms, a stimulus is applied at the bottom end of the cell by increasing calcium concentration to 50 μM, with (a) D_{NE} = 0.1 $\mu m^2/s$, (b) D_{NE} = 1.0 $\mu m^2/s$, (c) D_{NE} = 5.0 $\mu m^2/s$.

Dupont, G. et al, (1996) Am. J. Physiol. 271: C1390-C1399.

Yang, Z. and Steele, D.S. (2005) Circ. Res. 96: 82-90.

Li, P. et al, (2007) FIMH 2007, LNCS 4466, pp. 180-189.

P. Li is supported by ORSAS, Tetley and Lupton Scholarship and IRS (International Research Scholarship). This work was supported by the European Union through the Network of Excellence BioSim, Contract No. LSHB-CT-2004-005137.

Where applicable, the authors confirm that the experiments described here conform with The Physiological Society ethical requirements.

PC2

4-Aminopyridine-sensitive Ca^{2+} store in frog ventricle

A. Bhaskar[1], P.K. Subbanna[2], J.P. Rao[3] and S. Subramani[1]

[1]Physiology, CMC, Vellore, India, [2]Pharmacology, CMC, Vellore, India and [3]Physiology, KMC, Manipal, India

It is believed that a functionally significant intracellular Ca^{2+} store is absent in frog ventricle and that they depend on extracellular Ca^{2+} for contraction [1]. A series of findings in our lab has convinced us that there must be a functionally significant Ca^{2+} store in frog ventricle. Based on a previous report, we used 4-aminopyridine (4-AP), on frog ventricular strips [2].

Hearts were isolated from frogs (*Rana hexadactyla*) which were anesthetized with ether and pithed. 2 mm thick ventricular strips were prepared and mounted in a temperature controlled (25-28 °C) bath perfused with oxygenated solution of the following composition (in mmol L^{-1}): 117 NaCl, 3 KCl, 1 $CaCl_2$, 1 $MgCl_2$, 0.2 NaH_2PO_4, 0.8 Na_2HPO_4, 10 glucose, pH 7.4. Free end of the strip was connected to a force-transducer and force of contraction was recorded on a computer. The strip was paced with field

stimulation by silver electrodes at 0.2 Hz. Force of contraction was allowed to stabilize for over 30 minutes. Then the tissue was kept quiescent in a Ca^{2+} free solution (containing 0.2 mmol L^{-1} EGTA) with normal Na^+, low Na^+ or zero Na^+ (NaCl replaced with LiCl) for 10 minutes. Addition of 16 mmol L^{-1} 4-AP to the bath, produced contractures in all three Ca^{2+} free solutions. Effect of 4-AP was reversible. Contractures were significantly larger (P=0.006, n=6, Mann-Whitney U test) in zero Na^+ solution as compared to normal Na^+ solution. Effect of 4-AP was independent of K^+ channel blocking effect, since another K^+ channel blocker, TEA (16 mmol L^{-1}) was unable to produce contracture. 4-AP was able to produce contractures even in Ca^{2+} free solutions with 10 µmol L^{-1} Nifedipine, thereby proving that the contractures are due to Ca^{2+} released from an internal store and not due to extracellular Ca^{2+}.

In conclusion, 4-AP is able to release Ca^{2+} from an intracellular store in frog ventricle. Contractures were larger on inhibition of Ca^{2+} extrusive mode of Na^+-Ca^{2+} exchanger (NCX). This shows that NCX is an important Ca^{2+} clearing mechanism in frog ventricle. Effect of 4-AP is independent of K^+ channel blocking action. 4-AP is known to release Ca^{2+} from endoplasmic reticulum of neurons by activating phospholipase C/$InsP_3$ pathway [3]. This may not be the cause of contracture as neomycin pretreatment was unable to prevent contractures. It is also known that there are no $InsP_3$ receptors in frog ventricular myocardium [1]. Another known effect of 4-AP is sarcoendoplasmic reticulum Ca^{2+}-ATPase (SERCA) inhibition [4]. SERCA is present in frog ventricule and hence the cause for contracture could be SERCA inhibition.

Tijskens P et al. (2003). Biophys J **84**, 1079-1092.

Ozgul M et al. (2000). J Basic Clin Physiol Pharmacol **11**, 57-62.

Grimaldi M et al. (2001). J Neurosci **21**, 3135-3143.

Ishida Y & Honda H (1993). J Biol Chem **268**, 4021-4024.

We are grateful to the help and support given by staff, CMC, Vellore.

Where applicable, the authors confirm that the experiments described here conform with The Physiological Society ethical requirements.

PC3

Subcellular localization of β_1 adrenergic receptors and HCN4 channels in murine sinoatrial myocytes

P. Akella, J. Vega and C. Proenza

Physiology & Neurobiology, University of Connecticut, Storrs, CT, USA

The sympathetic nervous system accelerates heart rate via β adrenergic receptors (βARs) on sinoatrial node (SAN) myocytes. Knockout studies suggest that the β_1AR subtype mediates adrenergic control of heartrate in the mouse.[1,2] Hyperpolarization-activated cyclic nucleotide sensitive (HCN) channels are thought to be among the downstream effectors for this chronotropic effect. HCN4 is the main HCN channel isoform in the SAN.[3] We hypothesized that close association between β_1ARs and HCN4 channels would facilitate the rapid and efficient signaling that is critical for sympathetic control of heartrate. Here we have used immunofluorescent confocal microscopy to examine the distribution of β_1ARs and HCN4 channels on SAN cells.

Adult male mice were anesthetized with isoflurane and euthanized according to a University-approved protocol. SAN tissue was digested in a Ca^{2+}-free enzymatic cocktail and cells dissociated with a fire polished glass pipette. Following gradual reintroduction of Ca^{2+}, cells were plated onto poly-L-lysine coverslips, fixed with 4% paraformaldehyde, and permeabilized with 0.2% Triton X-100. Rabbit polyclonal primary antibodies against HCN4 (Alomone) or β_1AR (Santa Cruz) were applied at 4^{oC} overnight, and visualized with an Alexa488-conjugated goat anti-rabbit secondary antibody (Molecular Probes). Optical sections (0.5 µm) were acquired with a 100x oil objective on a Leica TCS SP2 laser scanning confocal microscope. Antibody specificity was confirmed by Western blotting of lysates from mouse atria or from CHO cells transfected with β_1AR, β_2AR, HCN2, or HCN4. Other controls included antibody preadsorption with antigenic peptides and omission of primary antibodies. All data represent at least three independent experiments.

Both HCN4 and β_1AR were conspicuously located on SAN cell membranes at discrete sites that appeared to be regions of contact between adjacent myocytes. HCN4 and β_1AR immunofluorescence was seen in lateral membrane regions and at the ends of the cells. These patterns was present in both larger, presumed "transitional," cells and in smaller, more slender "primary" cells. Additional HCN4 fluorescence was seen along the entire cell membrane, and additional β_1AR fluorescence was seen in puncta across the cell surface. In pairs of joined cells, there was marked β_1AR or HCN4 fluorescence at the cell-cell interface (Figure 1). These data suggest that HCN4 and β_1ARs are both localized at intercellular junctions between myocytes in the SAN.

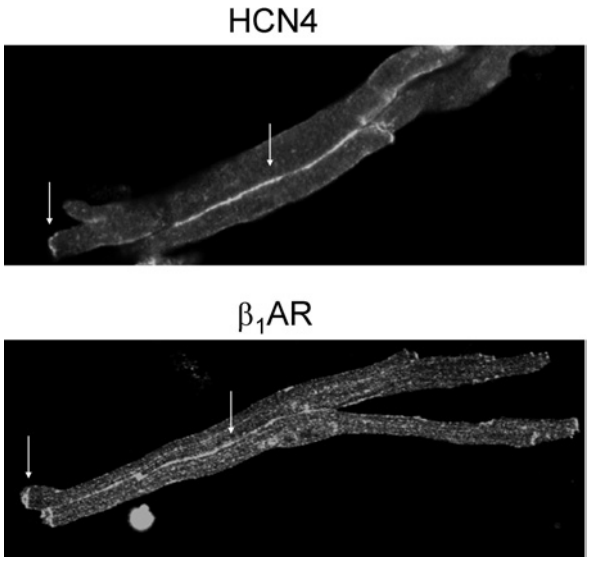

Figure 1. Pairs of sinoatrial myocytes labeled with anti-HCN4 (top) or anti-β_1AR (bottom) primary antibodies and an Alexa488-conjugated secondary antibody. Arrows indicate immunofluorescence at the ends of myocytes and at the interface between the cells.

1. Chruscinski, A.J. et al. (1999). J. Biol. Chem. 274, 16694-16700.

2. Rohrer, D.K. et al. (1996). PNAS 93, 7375-7380.

3. Moosmang, S. et al. (2001). Eur J Biochem 268, 1646-1652.

Where applicable, the authors confirm that the experiments described here conform with The Physiological Society ethical requirements.

PC4

Requirement of Popdc genes for sinus node function

T. Brand[1], A. Froese[1], C. Waldeyer[2], J. Schlueter[1], B. Kirchmaier[1], S. Breher[1], A. Torlopp[2], S.K. Liebig[2], S. Laakmann[2], J. Neumann[4], C. Winkler[5], P. Kirchhof[3], F. Vauti[5], H. Arnold[2] and L. Fabritz[1]

[1]Cell & Developmental Biology, University of Würzburg, Würzburg, Germany, [2]Department of Cardiology and Angiology, University Hospital Münster, Münster, Germany, [3]Institute of Pharmacology, University of Halle, Halle, Germany, [4]Physiological Chemistry I, University of Würzburg, Würzburg, Germany and [5]Cell- & Molecular Biology, TU Braunschweig, Braunschweig, Germany

The Popeye domain containing (Popdc) genes encode membrane proteins with a preferential expression in striated muscle. In vertebrates three genes are present in the genome of which Popdc2 expression is largely restricted to the heart, while Popdc1 and -3 are more widely expressed. In order to analyze their function we have created Popdc1 and Popdc2 null mutant mice by creating lacZ knock-in mutations. Both mouse strains displayed normal viability during postnatal life. Detailed analysis of the LacZ expression pattern of both mutants revealed a strong expression in the cardiac conduction system in the postnatal heart. Electrophysiological analysis of both mutants revealed conduction abnormalities. Popdc1 mice displayed a sinus bradycardia and a retarded AV node conductivity, which became pronounced after beta-adrenergic stimulation. Popdc2 developed a load-induced sinus bradycardia after subjecting mutant mice to an exercise test or to prolonged mental stress by airjet. The stress-induced bradycardia in Popdc2 mice was due to a sinus bradycardia and not due to prolonged AV conduction or AV nodal block. Interestingly, the bradycardic phenotype developed over time and was not present at 2 month of age, at 5.5 month significant differences between mutants and wildtype animals was observed in case of the exercise test, while at 9 month both exercise and mental stress elicited a bradycardic response. Histological analysis revealed structural defects in sinus node morphology. Hcn4 expression was reduced in the mutant and sinus node cells appeared to be progressively substituted by working myocardium. In support of this view the sinus node of Popdc2 mutant displayed co-expression of Cx30.2 and Cx43. Knockdown of popdc2 in zebrafish embryos revealed an essential function of popdc2 for cardiac and skeletal muscle development. Injected embryos displayed a disorganized tail musculature and a dysmorphic heart. At low morpholino concentrations some of the morphant's hearts displayed irregular cardiac contractions, a phenotype that is reminiscent of the conduction abnormalities observed in the mutant mouse heart. In conclusion the Popdc family plays an important role for heart and muscle development in zebrafish and is essential for the conduction system function in the adult mouse heart.

Supported by DFG, BR1218/10-4

Where applicable, the authors confirm that the experiments described here conform with The Physiological Society ethical requirements.

PC5

Cardiac pacemaker function of HCN4 channels is confined to embryonic development and requires cyclic AMP

D. Harzheim[1,2], R. Seifert[2], H. Pfeiffer[2], L. Fabritz[3], E. Kremmer[4], T. Buch[5], A. Waisman[6], P. Kirchhof[3] and U.B. Kaupp[2]

[1]Molecular Signalling, Babraham Institute, Babraham, Cambridge, UK, [2]Research Center Juelich, Juelich, Germany, [3]University Hospital Muenster, Muenster, Germany, [4]GSF, Muenchen, Germany, [5]University Zuerich, Zuerich, Switzerland and [6]Johannes Gutenberg University, Mainz, Germany

Important targets for cAMP signalling in the heart are hyperpolarization-activated and cyclic nucleotide-gated (HCN) channels that underlie the depolarizing "pacemaker" current, I_f [1, 2]. We studied the role of I_f in mice, in which binding of cAMP to HCN4 channels was abolished by a single amino-acid exchange (R669Q). Homozygous $HCN4^{R669Q/R669Q}$ mice die during embryonic development between embryonic day 11.5 and 12 (E11.5-12). Prior to E12, homozygous and heterozygous embryos display reduced basal heart rates (table 1) and show no or attenuated responses to catecholaminergic stimulation. Isoproterenol (1 μM) superfusion increased the rate of isolated hearts from $HCN4^{+/+}$ and $HCN4^{+/R669Q}$ embryos (37.4 ± 4.5 %, n = 8, and 19.8 ± 2.8 %, n = 6, respectively), whereas no increase was observed in hearts from $HCN4^{R669Q/R669Q}$ embryos (2.8 ± 2.5 %, n = 5). The genotypic differences in heart rate closely relate to differences in the respective I_f current. Electrophysiological studies on cardiomyocytes from $HCN4^{R669Q/R669Q}$ embryos revealed that the activation curve of I_f is shifted negatively. The voltage of half-maximal activation ($V_{1/2}$) in the three genotypes was -82.3 ± 3.2 mV (n = 12) for wild-type, -89.1 ± 6.6 mV (n = 12) for heterozygous, and -95.5 ± 4.5 mV (n = 9) for homozygous cardiomyocytes. Moreover, the $V_{1/2}$ in homozygous cardiomyocytes cannot be moved towards more positive values by the addition of cAMP (500 μM).

While heterozygous embryos display an obvious cardiac phenotype, adult $HCN4^{+/R669Q}$ mice display normal heart rates at rest and during exercise. However, following exercise, hearts exhibit pauses and sino-atrial node block.

We conclude that in the embryo, HCN4 is one of the principal cardiac pacemakers and persistent elevation of the heart rate by cAMP is essential for viability. In adult mice, HCN4 channels take no longer part in heart rate regulation, but prevent sinus pauses during and after stress. Thus, in mice, the mechanism of pacemaking switches during development and HCN4 may serve two different functions that both critically rely on the presence of cAMP.

Data are expressed as mean ± SEM.

Basal embryonic heart rate (bpm)

	E9.5	E10.5	E11
$HCN4^{+/+}$	164.5 ± 5.7 (n = 24)	174.6 ± 7.9 (n = 15)	194.5 ± 8.9 (n = 7)
$HCN4^{+/R669Q}$	128.7 ± 8.3 (n = 12)	128.0 ± 7.9 (n = 10)	141.0 ± 5.3 (n = 4)
$HCN4^{R669Q/R669Q}$	99.3 ± 7.4 (n = 6)	75.6 ± 8.3 (n = 5)	72.8 ± 6.5 (n = 6)

DiFrancesco, D. and P. Tortora (1991) Nature. 351(6322),145-147

Barbuti, A., M. Baruscotti, and D. Difrancesco (2007) Journal of Cardiovascular Electrophysiology 18(3), 342-347

D.H. was a fellow of the Boehringer Ingelheim Fonds, T.B. was supported by the Land Nordrhein-Westfalen, and P.K. is supported by the IZKF Münster.

Where applicable, the authors confirm that the experiments described here conform with The Physiological Society ethical requirements.

PC6

A novel mechanism of sphingosine 1-phosphate signalling in regulation of L-type Ca^{2+} channel activity in cardiac myocytes

E. Eroume A Egom, Y. Li, H. Musa and M. Lei

Division of Cardiovascular and Endocrine Sciences, University of Manchester, Manchester, UK

Sphingosine 1-phosphate (S1P) is bioactive lipid derived from metabolism of sphingomyelin that has been implicated in regulation of many cellular functions including ion channel activities (Hla, 2000; Pyne, 2000). To determine the effect of S1P on L-type calcium current (ICa,L) at basal and β-adrenergic stimulation conditions and underlying intracellular signalling pathways in rat ventricular cardiac myocytes, Western blot, immunocytochemistry and voltage patch clamping were used. The results are presented as mean ± SEM. Analysis was performed using the paired or un-paired Student's t test as appropriate and significance was accepted at $p < 0.05$. At basal condition, perfusion of S1P (100nM) had no significant effect on ICa,L (n=6, $p>0.05$). The effect of S1P on ICa,L was then studied in the presence of β-adrenergic stimulation by perfusion of 100 nM isoproterenol (ISO), a β-adrenergic receptor agonist. ICa,L was significantly enhanced in the presence of 100 nM ISO, the peak current density at 0 mV increased by 83.27 ± 2.8% from -3.44 ± 0.07 at the basal condition to -20.57 ± 0.76 pA/pF in the presence of ISO ($p < 0.01$, n = 7). ISO had a significant positive effect on ICa,L. Additional 100 nM S1P significantly blunt effect of ISO on ICa,L (in the presence of ISO), the peak current density at 0 mV increased by 68.99 ± 3.4% from -3.44 ± 0.07 to -11.1 ± 1.80 pA/pF ($p < 0.01$, n = 7). Our immunocytochemistry results also showed the co-localization between PAK1 (p21 activated kinase) - PP2A (protein phosphatase 2A) (n=25, $p<0.001$). Western blotting showed that the S1P1 receptor expressed in the cells whereas no visualization of S1P2 and S1P3 signals were observed. In conclusion, in rat ventricular myocytes, S1P does not affect the basal activity of L-type Ca channels but reversed the effect of the β-adrenergic agonist ISO on this channel. This effect is probably through PAK1-PP2A-mediated signalling pathway via S1P1 receptor.

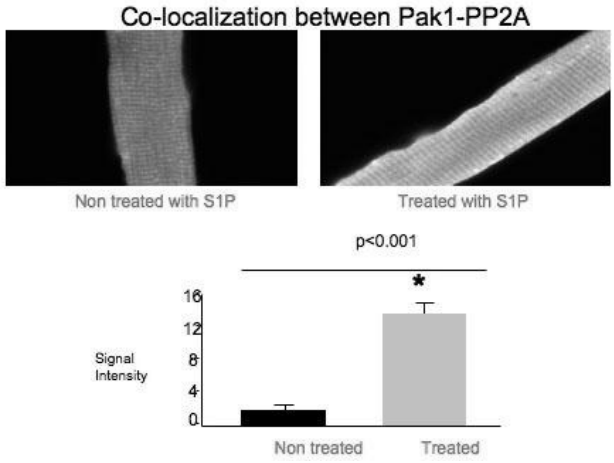

Figure 1.

Hla T, Lee MJ, Ancellin N, Thangada S, Liu CH, Kluk M, Chae SS, Wu MT (2000). Ann N Y Acad Sci 905, 16-24.

Pyne S, Pyne NJ (2000). Biochem J 349, 385-402.

This study was supported by the School of Medicine, University of Manchester and the Wellcome Trust. We thank Prof Mark Boyett group and Dr Jacqueline Ohanian for their support.

Where applicable, the authors confirm that the experiments described here conform with The Physiological Society ethical requirements.

PC7

Differential effects of ischemia and post-ischemia application of β-adrenergic agonists in neonatal AV and SA nodal cells during reperfusion – a potential mechanism for Junctional Ectopic Tachycardia?

Y. Qu[1,2], X. Sheng[1,2], P. Dan[1,2], E.A. Accili[4], S. Sanatani[3] and G.F. Tibbits[1,2]

[1]Child and Family Research Institute, Vancouver, BC, Canada, [2]Simon Fraser University, Burnaby, BC, Canada, [3]BC Children and Women's Hospital, Vancouver, BC, Canada and [4]University of British Columbia, Vancouver, BC, Canada

Cardiopulmonary bypass (CPB) is associated with an ischemia-reperfusion injury which can potentially impact the rhythmicity of the heart. Junctional Ectopic Tachycardia (JET) is the most common post-operative arrhythmia seen in neonates and infants undergoing CPB for repair of heart defects. Clinical evidence suggests JET originates from the AV node area and ischemia is speculated to be a pathogenic factor. JET is also associated with the post-operative administration of inotropes, in particular dopamine.

To determine how ischemia-reperfusion affects the pacemaker cell activity in neonates, AV nodal (AVNC) and SA nodal cells (SANC) were isolated from 10-day old New Zealand white rabbits and spontaneous action potentials were recorded using the perforated current clamp technique. Rabbits were anesthetized with thiopental sodium (60mg/kg) through intra-peritoneal injection prior to thoracotomy. The heart was rapidly excised and perfused with collagenase and subsequently protease in the Langendorff mode. AVNCs were dissociated from the AVN tissue cut at the triangle of Koch. SANCs were dissociated from the SAN tissue located adjacent to the crista terminalis. AVNCs and SANCs were identified by their automaticity, input resistance, and pacemaker current expression. We recorded APs during pre-ischemia, ischemia, post-ischemia with drugs and reperfusion with normal Tyrode's solution.

After 5 min exposure to the ischemia solution (pH 7.0, 5 mM lactate, 0 mM glucose), action potential (AP) frequency on AVNCs decreased and the AP duration was shortened ($p<0.05$, n=8, paired-samples t test); ischemia had no significant effect on SANCs over the same time period. Our results showed 20 μM dopamine consistently led to irreversible irregular APs during reperfusion on AVNCs (n=4) but not on SANCs. Typical changes in AP pattern were: slower upstroke, unstable maximal diastolic potentials, and an increase in early and delayed afterdepolarizations (EAD and DAD). Isoproterenol (1 μM) also induced AP

changes in AVNCs (n=3) during reperfusion but to a lesser extent, without EAD but with DAD.
We conclude AVNCs are more susceptible to ischemia than SANCs in neonates; we also demonstrate that the post-ischemia application of β-adrenergic agonists may exacerbate the trauma from ischemia and lead to irregular electrical activity in AVNCs during reperfusion. Whether JET results from a deterioration of AV conduction or abnormally enhanced AV automaticity needs to be explored further.

Where applicable, the authors confirm that the experiments described here conform with The Physiological Society ethical requirements.

PC8

Computational evaluation of the effects of novel anionic currents on human atrial electrical behaviour

S. Kharche[1], J. Stott[1], P. Law[1], H. Zhang[1] and J.C. Hancox[2]

[1]School of Physics and Astronomy, University of Manchester, Manchester, Lancashire, UK and [2]Department of Physiology, Bristol Heart Institute, Bristol, UK

A novel outwardly rectifying anionic background current (I_{ANION}) with small conductance (≤0.4 pS/pF) has been recently identified in human atrium [1], which can contribute to shortening of atrial action potential duration (APD) during phase 2 repolarisation period. In this study, we computationally evaluated the functional effects of I_{ANION} on atrial electrical excitation-wave propagation and conduction in humans.
The cellular model of human atrial action potentials (APs) by Courtemanche *et al.* [2] was modified to incorporate I_{ANION}, with either nitrate or chloride ($NO3^-$ or Cl^-) ions as charge carriers [1]. The model was used to investigate the effects of the anionic background current on effective refractory period (ERP), and AP and ERP restitutions. The single cell model was then incorporated into a homogenous multicellular model of human atrial tissue we developed in a previous study [3] to investigate the effects of the anionic current on intra-atrial conduction velocity restitution, tissue's vulnerability to re-entry and characteristics of re-entrant excitation waves, such as the frequency, lifespan and tip meandering pattern of re-entry.
Previous work has shown that inclusion of $I_{ANION(Cl)}$ or $I_{ANION(NO3)}$ in the Courtemanche *et al.* model had only a minor (~1 mV) effect on atrial resting membrane potential and at an AP frequency of 1Hz I_{ANION} abbreviated atrial APD_{50} by ~10% with Cl^- and ~13.5% with $NO3^-$ as charge carrier without abbreviation of APD_{90} [1]. The present simulations showed that, paradoxically, incorporation of I_{ANION} prolonged atrial ERP at a pacing cycle length of 1000 ms and flattened APD_{90} the restitution curve. I_{ANION} facilitated atrial conduction manifested by an increase in conduction velocity. I_{ANION} also increased atrial tissue vulnerability to genesis of re-entry (by 8.7 % for $I_{ANION(Cl)}$ and 8.4 % for $I_{ANION(NO3)}$) in response to a premature stimulus applied to the refractory tails of a conditioning wave, because of facilitated inter-atrial conduction. Tip meandering pattern of re-entrant excitation waves was unaffected, decreased the frequency of electrical excitations, and increased the lifespan of the re-entry.
Our simulations show that the outwardly rectifying anionic background current I_{ANION}, though small, nevertheless influences atrial electrical AP morphology, APD, ERP and their rate dependencies. It affects intra-atrial conduction, tissue's vulnerability to genesis of re-entry and dynamic behaviours of re-entrant excitation waves.

Li H, Zhang H, Hancox JC, Kozlowski RZ (2007). Biochem Biophys Res Commun 359, 765-70.

Courtemanche M, Ramirez RJ & Nattel S (1998). Am J Physiol 275, H301-H321.

Kharche S, Seemann G, Leng J, Holden A.V., Garatt C J, Zhang H (2007). LNCS 4466, 129-138.

Biktasheva IV, Biktashev VN & Holden AV (2005). LNCS 3504, 293-303.

This work was supported by BHF (140/PG/03).

Where applicable, the authors confirm that the experiments described here conform with The Physiological Society ethical requirements.

PC9

Reduced conduction velocity caused by class Ib anti-arrhythmic drugs contributes to both their anti- and pro-arrhythmic effects in human virtual ventricular tissues

J.A. Lawrenson[1], A.P. Benson[2] and A.V. Holden[2]

[1]School of Medicine, University of Leeds, Leeds, UK and [2]Institute of Membrane and Systems Biology, University of Leeds, Leeds, UK

Ventricular tachycardia and fibrillation are dangerous cardiac arrhythmias. Anti-arrhythmic drugs such as lidocaine (a class 1b drug) can prevent such arrhythmias, but they have pro-arrhythmic side effects whose mechanisms are poorly understood. We used computational models to elucidate these mechanisms.
Effects of lidocaine were simulated (1) in human ventricular cell models (2). The drug binds to the inactivated state of the sodium channel and has on and off rate constants of 31.0 /mM/s and 0.79 /s respectively, as measured experimentally in human ventricular cells (3). These drug effects were incorporated into 75 mm one-dimensional (1-D) heterogeneous transmural, and 12×12 cm two-dimensional (2-D) epicardial, virtual tissues (4). Drug effects were characterised and validated in single cell models. Simulated application of 0.08 mM lidocaine produced rate-dependent steady state (end systolic) block of the sodium current I_{Na} and reductions in maximum action potential upstroke velocity dV/dt_{max} (Table 1). There was little effect on action potential duration (APD). This is consistent with (5). In 1-D tissues, the reduced upstroke velocity under drug conditions caused reduced conduction velocity, and propagation block at short cycle lengths (CLs). The reduced conduction velocity was associated with an increased vulnerable window for unidirectional propagation (4). The maximum temporal width of the vulnerable window, expressed as a percentage of the diastolic interval, increased with pacing rate and simulated drug concentration, from 1% at CL = 1000 ms with 0.015 mM lidocaine to 18% at CL = 500 ms with 0.2 mM lidocaine. In 2-D virtual tissues, this reduced conduction velocity prevented initiation of re-entry (tachycardia), prevented breakdown of re-entry into fibrillation, or shortened the lifetime of re-entry, depending on simulated drug concentration.
We conclude that the anti-arrhythmic mechanism of class Ib drugs in the virtual tissues is reduced conduction velocity, and

propagation block at the high rates of excitation seen during arrhythmias. The pro-arrhythmic mechanism is an increase in the vulnerable window for unidirectional propagation, also caused by the reduced conduction velocity.

Table 1. Effects of simulated application of 0.08 mM lidocaine. All values are percentages.

	CL = 500 ms			CL = 1000 ms		
	Block of I_{Na}	$\Delta dV/dt$ max	ΔAPD	Block of I_{Na}	$\Delta dV/dt$ max	ΔAPD
Endocardial	65.9	-44.9	+2.5	53.2	-35.6	+1.7
Midmyocardial	69.6	-46.9	+0.7	56.4	-38.0	+0.6
Epicardial	66.0	-44.7	+0.9	53.3	-35.6	+0.8

Starmer CF *et al.* (1991). *Circulation* **84**, 1364-1377.

Ten Tusscher KHWJ & Panfilov AV (2006). *Am. J. Physiol.* **291**, H1088-H1100.

Furukawa T *et al.* (1995). *J. Mol. Cell. Cardiol.* **27**, 831-846.

Holden AV *et al.* (2006). *J. Biol. Phys.* **32**, 355-368.

Weirich J & Antoni H (1998). *Basic Res. Cardiol.* **93**, 125-132.

Supported by Heart Research UK (JAL) and the Dr Hadwen Trust for Humane Research (APB).

Where applicable, the authors confirm that the experiments described here conform with The Physiological Society ethical requirements.

PC10

Pharmacological characterisation of nine single nucleotide polymorphisms of the human ether-a-go-go-related gene-encoded potassium channel

R. Mannikko[1], A.R. Harmer[1], G. Overend[2], C. Perrey[2], J. Valentin[1], J. Morten[2], M. Armstrong[2] and C.E. Pollard[1]

[1]Safety Assessment UK, AstraZeneca R&D, Alderley Park, Macclesfield, Cheshire, UK and [2]R&D Genetics, AstraZeneca R&D, Alderley Park, Macclesfield, Cheshire, UK

Early in drug discovery the IC50 of compounds blocking the human ether-a-go-go-related gene (hERG)-encoded channel is used to assess drug-induced QT interval prolongation risk. We do this using the Caucasian wild-type (WT) variant & assume its pharmacology is the same as that of variants that exist in patient populations. Our objective was to test this assumption by defining the pharmacology of 9 hERG single nucleotide polymorphisms (SNPs) largely selected from Ackerman *et al.* (2003): R176W, R181Q, Del187-189, P347S, K897T, A915V, P917L, R1047L & A1116V.

Each SNP was expressed in Tet-On CHO K1 cells. Tail current amplitudes were measured using automated electrophysiology (IonWorks (IW)) to estimate the potency of 48 hERG blockers, mostly those reviewed by Redfern *et al.* (2003).

In phase 1 of the work each WT-SNP comparison was made on the same day but not in the same IW test-plate. IC50s were estimated by fitting to an 8-point, non-cumulative concentration-effect curve made up of 32-48 data points & expressed as a mean IC50; lower, upper 95% confidence limit (CL)). This gave 432 WT-SNP IC50 comparisons (48 compounds X 9 SNPs) expressed as △IC50 values. These values ranged from 4-fold (potency at SNP ⟩WT) to 3-fold in the opposite direction. For 77 compound-SNP combinations the WT upper or lower CL did not overlap with the SNP's.

In phase 2 each of these 77 cases was re-examined in the same IW test-plate to minimise variability. Using this design, 62 no longer yielded IC50 values with non-overlapping CLs. For 7 of the remaining 15 cases there were again non-overlapping CLs but this time in the opposite direction. Thus for only 8 compound-SNP combinations were there IC50s with non-overlapping CLs in the same direction as for the first phase (△IC50 values were never ⟩2-fold).

The absence of large △IC50 values was unrelated to the IW-based assay system, since using a hERG drug-binding site mutant (Y652A) propafenone was 6-fold less potent (IC50 3.84; 3.46, 4.26 μM) than WT (IC50 0.65; 0.59, 0.75 μM), the same fold-shift reported by Witchel *et al.* (2004) using conventional electrophysiology.

In summary, potencies defined using the Caucasian WT sequence, at least in this *in vitro* system, are representative of potencies for these relatively common SNPs. We cannot completely exclude the possibility that there are small differences in pharmacology for a few compound-SNP combinations, but such differences cannot confidently be distinguished from assay variability. However, there remains the possibility that these SNPs influence the pharmacology or other hERG channel characteristics *in vivo*.

Ackerman MJ *et al.* (2003). *Mayo. Clin. Proc.*, **78**, 1479-1487.

Redfern WS *et al.* (2003). *Cardiovasc. Res.*, **58**, 32-45.

Witchel HJ *et al.* (2004). *Mol. Pharmacol.*, **66**, 1201-1212.

Where applicable, the authors confirm that the experiments described here conform with The Physiological Society ethical requirements.

PC11

ATP (P2) receptor expression in the sinoatrial node

H. Musa, J.O. Tellez, I.D. Greener, H. Dobrzynski and M.R. Boyett

School Of Medicine, University Of Manchester, Manchester, UK

ATP and its derivatives are known to exert profound electrophysiological effects on the heart. Recent studies have revealed the expression of various P2 receptors, both ligand-gated P2X receptors and G-protein coupled P2Y receptors, throughout the heart. Although it is possible that they play a significant role in pacemaker activity (Ju et al., 2003), there are no detailed reports on the expression of the P2 family in the sinoatrial node (SAN). To investigate the expression profile of P2 receptors, we used quantitative PCR (qPCR) to measure the abundance of P2 receptor mRNA in the sinoatrial node (and also atrium and ventricle) of Wistar-Hannover rats (n=7). qPCR was carried out using an ABI 7900HT instrument together with ABI Taqman probe assays. In addition, we confirmed P2 receptor mRNA expression using in situ hybridisation (ISH) and measured protein expression using Western blotting. ISH was performed with a transcript specific riboprobe and Western blotting was performed with a transcript specific antibody (Alomone Labs). qPCR revealed the presence of mRNA for P2X receptors 1, 2, 3, 4, 5 and 7 (6 was not expressed) and P2Y receptors 1, 2, 4, 6, 12, 13 and 14 (11 was not tested) in the three areas of the heart. Of the transcripts

investigated, P2X5 mRNA was 10 fold more abundant than any other transcript, in all tissue areas. P2X5 mRNA abundance was approximately the same as HCN4 (the primary alpha-subunit for the pacemaker current If) mRNA in the SAN. ISH was performed to confirm that the P2X5 mRNA was expressed in myocytes (rather than intra-cardiac neuronal tissue for example): a P2X5 specific riboprobe revealed strong specific labelling around the nuclei (site of the rough endoplasmic reticulum) in the sinoatrial node (Fig. 1A, arrow) and the atrial muscle (Fig. 1B); labelling was similar in the two regions, in agreement with the qPCR data. Labelling was also present within blood vessels (Fig. 1B, arrows). Finally, Western blot was carried out to determine whether the protein is present: a P2X5 specific antibody produced a single band at the expected molecular weight (51 kD) in all tissues. These data show the presence of mRNA for various P2 receptors in the sinoatrial node (and also atrium and ventricles). Whether P2X5 (the most abundant of the receptors) plays a significant role in pacemaking in the sinoatrial node remains to be elucidated.

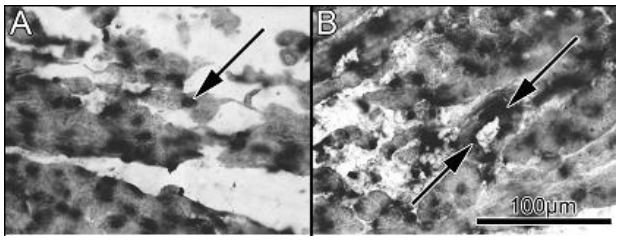

Figure 1. A, P2X5 mRNA expression in the sinoatrial node. B, P2X5 mRNA expression in the atrial muscle of the crista terminalis.

Ju YK, Huang W, Jiang L, Barden JA, & Allen DG (2003). J Physiol 552, 777-787.

Where applicable, the authors confirm that the experiments described here conform with The Physiological Society ethical requirements.

PC12

Acidosis delays conduction through the atrioventricular node

A.M. Nisbet[1], M. Craig[1], N.L. Walker[1], F.L. Burton[1], S.M. Cobbe[1], J. Hancox[2], C. Orchard[2] and G.L. Smith[1]

[1]BHF Glasgow Cardiovascular Research Centre, University of Glasgow, Glasgow, UK and [2]University of Bristol, Bristol, UK

The effects of acidosis on the electrophysiology of the sinoatrial (SAN) and atrioventricular (AVN) nodes were investigated. Hearts from adult male New Zealand White rabbits were excised under terminal anaesthesia. In one series of experiments (n=6), optical mapping was used to image left ventricular activation in Langendorff-perfused rabbit hearts stained with the voltage-sensitive dye RH237 and paced from the right atrium (RA). Left ventricular epicardial activation was recorded at 16x16 sites in a 2x2cm square. In another series (n=11), SAN cycle length (CL) and AVN conduction were studied in an isolated right atrial/AVN preparation, containing the triangle of Koch and crista terminalis, superfused with Tyrode's solution at 37°C. Extracellular electrodes recorded atrial and His bundle signals during sinus rhythm or pacing from the crista terminalis. Atrio-Hisian (AH) interval, Wenckebach cycle length (WCL) and AVN functional (FRP) and effective (ERP) refractory period were derived from pacing protocols. Data were obtained at pH 7.4, 6.8 and 6.3 (Table 1). Comparisons of values at each pH increment were made using a paired t-test, and a two-tailed P-value of < 0.05 was considered statistically significant. In intact hearts, the time to earliest ventricular activation (TEact) following RA pacing prolonged as PCL shortened, consistent with delay originating at the AVN. Reduction of perfusate pH resulted in significant and reversible prolongation of TEact. In the isolated preparation, the spontaneous SAN CL lengthened with reduction of pH. There was reversible prolongation of the AH interval and WCL during acidosis, with significant prolongation of AVN FRP and ERP. In conclusion, acidosis prolongs the time to earliest ventricular activation from RA pacing due to a significant increase in AVN delay. Furthermore, acidosis prolongs the refractory period of the AVN and slows the SAN firing rate.

Table 1

	SAN CL	TEact300	TEact200	WCL	AH300	AH200	AVN FRP	AVN ERP
pH 7.4	420.5±24.4	85.9±5.9	100.8±6.8	198.2±21.5	45.8±3.1	76.0±26.2	205.1±21.7	176.8±22.0
pH 6.8	572.7±56.8*	109.6±4.4	116.5±16.0	268.3±29.4**	54.2±3.5*	90.9±24.6*	237.6±18.4**	210.7±16.9*
pH 6.3	720.2±59.6*	173.5±26.4*	189.4±39.1*	296.0±46.8*	68.5±7.4*	#	220.7±27.4*	209.3±30.6
pH 7.4 (return)	493.7±29.9	89.7±10.4	109.3±33.4	262.0±32.8	68.5±7.4	85.3±24.2	246.3±33.4	220.4±27.7

Data expressed as mean ± SEM (ms). TEact300 - TEact at PCL 300ms; TEact200 - TEact at PCL 200ms; AH300 - AH at PCL 300ms; AH200 - AH at PCL 200ms. *$p<0.05$, **$p<0.01$, # At pH 6.3 data was not included in analysis due to complete heart block at PCL 200ms in 9 of 11 samples.

Where applicable, the authors confirm that the experiments described here conform with The Physiological Society ethical requirements.

PC13

Characterizing a novel SCN5A mutation associated with sick sinus syndrome

J. Gui[1], Y. Zhang[2], T. Wang[3], T. Zimmer[4] and M. Lei[1]

[1]Cardiovascular Research Group, The university of Manchester, Manchester, UK, [2]Department of Cardiology, Xian Jiaotong University, Xian, China, [3]Medical Genetics Research Group and Centre for Molecular Medicine, The University of Manchester, Manchester, UK and [4]Institute of Physiology II, Friedrich Schiller University, Jena, Germany

The SCN5A gene, encoding human cardiac-type voltage-dependent Na+ channels (Nav1.5), is essential in initiation of cardiac activity. Genetic defect of SCN5A channel has been associated with a variety of inherited cardiac arrhythmic disorders(Benson et al., 2003; Shimizu, 2005; Modell & Lehmann, 2006; Wolf & Berul, 2006). We characterized a novel SCN5A mutation, R878C, in the second pore segment of SCN5A identified in a three-generation Chinese family associated with variable clinical expression of sick sinus syndrome and asymptomatic Brugdada Syndrome. SCN5A mutations were generated using site-directed mutagenesis and heterologously expressed in HEK293 cells. Whole-cell voltage clamp was used to record current and subcellular localization was determined by confocal imaging. Heterologous expression the WT channel in HEK293 cells showed average peak current density 95±6.2 pA/pF (n=15), while the

R878C cells (n=20) did not show any detectable current. There was also no detectable current of R878K (n=10) with lysine substituting arginine at amino acid 878, demonstrating that the positive change at 878 is not the only key defect for the mutant channel. Further immunocytochemistrical characterization revealed that mutant channel had normal trafficking to the plasma membrane, which suggested that the mutant channel produced a non-functional channel phenotype but had normal intracellular trafficking to the plasma membrane.

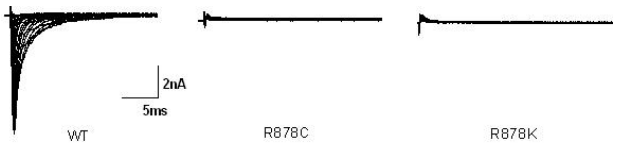

Effects of mutations on sodium channel

Benson DW, Wang DW, Dyment M, Knilans TK, Fish FA, Strieper MJ, Rhodes TH & George AL, Jr (2003). J Clin Invest 112, 1019-1028.

Modell SM & Lehmann MH. (2006). Genet Med 8, 143-155.

Shimizu W. (2005). Intern Med 44, 1224-1231.

Wolf CM & Berul CI. (2006). J Cardiovasc Electrophysiol 17, 446-455.

This work is funded by The Welcome Trust and Dorothy Hodgkin Postgraduate Award

Where applicable, the authors confirm that the experiments described here conform with The Physiological Society ethical requirements.

PC14

In rat and guinea-pig hearts, the retroaortic knot expresses the major isoform of the funny channel - HCN4

J.F. Yanni[1], M.R. Boyett[1], R.H. Anderson[2] and H. Dobrzynski[1]

[1]Cardic electrophysiology unit, Manchester University, Manchester, UK and [2]Cardiac Unit, Institute of Child Health, University College London, London, UK

It is well established that the atrioventricular (AV) conduction axis is the so-called "specialised" component of the junctions between the atrial and ventricular myocardial tissues, and that the bundle of His is the only muscular structure that, in the normal heart, crosses the plane of AV electrical insulation. It has remained controversial, however, as to whether other parts of the atrial vestibules are histologically specialised. Kent, in 1893, proposed that multiple muscular bridges cross from atrium to ventricle as the substrate for normal AV conduction. It is certainly the case that, in human hearts, remnants of histologically specialised myocardium are to be found on the atrial side of the insulating plane, albeit *without* making muscular connections with the ventricular myocardium, but the full extent of these so-called AV ring tissues has still to be established.

In the present study, using histology and immunoconfocal microscopy, we have investigated the specialised components of the AV junction in the hearts of four rats and guinea-pigs. The animals were humanely killed, and the hearts rapidly removed and frozen in liquid nitrogen. 20 μm serial sections were then cut through the entirety of the AV junctions.

In both species, extensive areas of histologically discrete myocardium are found in the vestibules of the tricuspid and mitral valves. The areas are more extensive in guinea-pig than rat, and show the immunohistochemical characteristics of pacemaker tissue. The best developed part of these specialised tissues, apart from the AV conduction axis itself, is found in the atrial septum immediately posterior to the aortic root, an area previously described as the retroaortic knot (RAK). Immunofluorescence and confocal microscopy revealed that, as with the AV conduction axis of the heart, this RAK tissue is positive for the major isoform of the funny channel, HCN4, and negative for the major gap junction channel, Cx43. In addition, the RAK tissue, like other cardiac myocytes, expresses caveolin3, a membrane bound protein. We used the expression of caveolin3 to measure the diameter of RAK cells. The RAK cells are significantly larger than AV node cells, but significantly smaller than atrial and ventricular cells (10.34 ± 0.99, 6.76 ± 0.38, 14.45 ± 0.61 and 18.92 ± 0.58 μm, respectively). In both species, the RAK is in continuity with the rings of specialised myocytes that encircle the orifices of the tricuspid and mitral valves.

We conclude that the ring tissues, including the RAK, expressing HCN4, may be capable of initiating spontaneous pacemaker activity, and could be a source of arrhythmias.

Kent AFS (1893). J Physiol 14, i2-254.

Where applicable, the authors confirm that the experiments described here conform with The Physiological Society ethical requirements.

PC15

A novel model of heart rate variability based on ion channel kinetics in the sinoatrial node

M. Nirmalan[1] and M. Niranjan[2]

[1]Intensive Care Unit, Manchester Royal Infirmary, Manchester, UK and [2]Department of Computer Sciences, University of Sheffield, Sheffield, UK

Rate of spontaneous depolarization in the sino-atrial node (SAN) is modulated by sympathetic and parasympathetic neural inputs. These interactions manifest as variations in instantaneous heart rate, commonly referred to as heart rate variability (HRV). Mathematical models of HRV should therefore be based on effects of the autonomic nervous system on ion channel kinetics responsible for SAN automaticity. We describe a model of HRV based on the above interactions.

Generation of pace maker potential was simulated using an 'integrate and fire' model, analogous to the charging of a capacitor via a resistor, starting from a resting membrane potential (RMP) of -50 mV to a reversal potential of -15 mV. When the potential reaches a threshold of -40 mV, the action potential is triggered. Two specific enhancements were made to the above basic model. Firstly, Phase 4 depolarization was assumed to occur in two stages: an initial slow exponential rise followed by a second accelerated exponential rise [associated with voltage independent late diastolic spontaneous Ca2+ release (1)]. Secondly, time constants for membrane depolarization at successive epochs were the product of linear interactions between (a) inherent stochasticity in channel activity and (b) sinusoidal inputs from the sympathetic

(0.1Hz) and parasympathetic (0.25Hz) efferents that increased and decreased the open probability of ion channels respectively. Average heart-rate (beats per minute) and variability (standard deviation as a percentage of mean heart rate) at varying levels of input from the sympathetic and parasympathetic systems are shown in Table 1. Maximal variability was seen when depolarization occured under both sympathetic and parasympathetic control (SD=34%). Variability was considerably lower when only one of the autonomic components was active (17%) and lowest when the heart was completely isolated from the autonomic inputs (0.1%).

We provide the first comprehensive model of HRV based on interactions between SAN ion channels and autonomic nerves. This model acknowledges two well recognized but, hitherto unexplained, features of HRV: namely (1) Low levels of HRV can be demonstrated in the absence of autonomic inputs (e.g isolated heart preparations); and (2) HRV is reduced during both sympathetic blockade (2) and sympathetic stimulation (3).

Sympathetic input	Parasympathetic input	Mean heart rate (bpm)	Variability SD as % of mean
0.0	0.0	60.0	0.13
0.0	1.0	43.4	16.7
1.0	0.0	89.0	17.4
1.0	1.0	61.0	33.9

Average heart rate and variability (SD of heart rate as a % of mean heart rate), under varying conditions of autonomic control

Vinogradova TM et al. (2004). Circulation Research 94, 802-809.

Lampert R et al. (2003). American Journal of Cardiology 91, 137-142.

Godin PJ et al. (1996). Critical Care Medicine 24, 1117-1124.

Where applicable, the authors confirm that the experiments described here conform with The Physiological Society ethical requirements.

PC16

Comparative physiology of the sinoatrial pacemaker of cold-blooded vertebrates

V.A. Golovko

Institute of Physiology, Komi Science Centre, Urals Branch, Russian Academy of Sciences, Syktyvkar, Russian Federation

It is known that the proximal and distal ends of the tubular heart of tunicates have two centres of automatism that work alternately. As a result, the blood advances by peristaltic contracting waves. Active animal living has led to the appearance of a bent tube with various chambers and valves between them. The pacemaker's cytoarchitecture also has changed. The aim of our study was to analyse the main parameters of the action potential (AP) in true pacemaker cells in the hearts of different poikilotherm species, including inhabitants of water (ammocoete, Lampetra fluviatilis, dace, Leuciscus rutilus) and land (frog, Rana temporaria, tortoise, Testudo horsfieldi). Experiments were carried out on spontaneously beating strips of sinoatrial (SA) tissue (control conditions: 20°C, 0.9 mM Ca^{2+}), using the standard microelectrode technique. In cold-blooded animals, in the evolutionary scale from Cyclostomata to Reptiles, true pacemaker cells are located along the full border between the sinus venosus and atrium. Two SA valves originated at this site and formed a roller called 'the sinoatrial ring'. These modifications changed the working regime of the vertebrate's electromechanical pump from a peristaltic one to an impulse one. When the isolated SA ring of the dace's heart was divided into two, the frequency of AP generation in the left and right segments was 69±11 min^{-1}, (n=11 strips) and 72±9 min^{-1} (n=11, $p>0.05$), respectively. However, the frequency of AP generation was higher (91±12 min^{-1}, $p<0.05$) in the non-divided isolated dace's SA ring. The action potential duration at 90% repolarization (APD_{90}) increased from the ammocoete (0.11±0.02 s, n=39 cells) to the tortoise (1.1±0.15 s, n=72). The rate of change of membrane potential (dV/dt) during phase 3 was highest in the ammocoete (1.2 V s^{-1}) and lowest in the tortoise (0.2 V s^{-1}). Interestingly, the SA pacemaker of different animal species appeared to be heterogeneous in its resistance to Ca^{2+}-free solution. In particular, the ammocoete's heart continued generating APs for longer than 10 hours in Ca^{2+}-free solution, while complete blockade of AP generation was observed in strips of the tortoise heart after 5 min of perfusion with 0.45 mM Ca^{2+} solution. We propose that many of the Ca^{2+}-dependent mechanisms of pacemaker function can be found even in more genetically primitive creatures such as Metazoa.

Where applicable, the authors confirm that the experiments described here conform with The Physiological Society ethical requirements.

PC17

Gi2 plays a critical role in the short-term modulation of heart rate dynamics

Z. Zuberi[1], L. Birnbaumer[2] and A. Tinker[1]

[1]Medicine, UCL, London, UK and [2]National Institute of Environmental Health Sciences, Research Triangle, NC, USA

Acetylcholine released from the vagus nerve acts on cardiac M2 receptors to cause negative chronotropic responses and this is due, in part to an increase in K^+ conductance mediated by G-protein inwardly rectifying potassium (GIRK)channels (Sakmann et al. 1983. This process is pertussis toxin sensitive implicating Gi/o in GIRK channel activation. Ablation of cardiac GIRK channels at a molecular level leads to impaired parasympathetic responses in vivo (Wickman et al. 1994). Giα2 is considered the most abundant cardiac isoform. We screened mice on an Sv129 background with global genetic deletions of Gαi2 and Gαi 1 and 3 as a double knockout with littermate controls (adjusted for age, weight and sex) and assessed negative chronotropic responses to intraperitoneal carbachol administration (500ng/g) under inhalation isoflurane anaethesia. Maximal relative inhibitory response was attenuated in Gαi2-deficient mice (mean inhibition 0.1152 ± 0.024, n=6) compared to control (0.3261 ± 0.054, n=6) or Gαi1/3 (0.3280 ± 0.080, n=6). Additionally, using heart rate variability analysis (HRV) of ECG data collected from implantable telemetry devices we were able to measure heart rate dynamics in conscious freely moving mice (Gehrmann et al. 2000). Our results suggest differential heart rate responses with respect to particular Giα isoform. Mean heart rate (HR) over 48hrs demonstrated that Gαi2 (-/-) deficient mice had significantly higher nocturnal HR (Gαi2, 617.6 ± 11.89 (n=5) vs control, 568.5 ± 14.64 (n=6) vs Gαi1/3, 579 ± 8.2 (n=6) (1-way

ANOVA, $P < 0.05$, n=6). Similarly day time heart rate showed a similar trend. We also examined HR dynamics in the short term in both frequency and time domains. Total power (TP), low frequency (LF) and high frequency (HF) spectral components of power were significantly reduced with respect to littermate controls and Gαi1/3 double knockouts (1-way ANOVA, $P < 0.05$, n=6). Similarly in the time domain mean N-N interval was signifcantly shorter in Gαi2 (-/-)-deficient mice than other groups. We next performed similar experiments in WT mice using the selective GIRK blocker tertiapinQ (Drici et al. 2000) or the muscaranic receptor antagonist atropine and reassessed HR dynamics. Our results suggest that both tertiapinQ and atropine have effects similar to global deletion of Gαi2 with respect to HRV. Additionally tertiapinQ pretreatment of WT (and Giα1/3) mice attenuates carbachol-induced bradycardia.

Sakmann B, Noma A & Trautwein W (1983). Nature 303, 250-253.

Wickman K, Nemec J, Gendler S & Clapham D (1998). Neuron 20, 103-114.

Gehrmann J, Hammer P, Maguire C, Wakimoto H, Triedman J & Berul C (2000). Am J Physiol 279, H733-H740.

Drici MD, Diochot S, Terrenoire C, Romey G & Lazdunski M (2000). Br J Pharmacol 131, 569-577.

This work was supported by the MRC and BHF.

Where applicable, the authors confirm that the experiments described here conform with The Physiological Society ethical requirements.

PC18

Histological and immunohistochemical characterisation of cells types in different regions of the human sinus node

N.J. Chandler[1], P. Molenaar[2], S. Birchall[1], H. Musa[1], V. Sharma[3], D.C. Sigg[3], M.R. Boyett[1] and H. Dobrzynski[1]

[1]Division of Cardiovascular and Endocrine Sciences, University of Manchester, Manchester, UK, [2]University of Queensland, Queensland, QLD, Australia and [3]Medtronic Inc., Minneapolis, MN, USA

We have shown that functionally and morphologically the rabbit sinus node (SN) is an extensive structure – it extends from the superior (SCV) to inferior (ICV) caval vein (1,2). It has also been shown that in the human, the leading pacemaker site can occur anywhere between the SCV and ICV (3). Therefore, the aims of this study were to determine if morphologically the human SN is a more extensive structure than previously thought and to investigate cell types within and around the SN.

Four healthy human SN/atrial specimens (not used for transplantation from Queensland Heart Valve Bank) were used. Serial frozen tissue sections were stained for histology (with Masson's trichrome stain) to locate the SN. Adjacent sections were immunolabelled with various antibodies to distinguish different population of cells within and around the SN. Cx43 (major connexin in the working myocardium) and ANP (atrial natriuretic peptide) were used as negative markers of nodal tissue; caveolin3 and vimentin were used as markers of cardiac cells and fibroblasts respectively. Western blotting was used to test the specificity of the antibodies. Scion Image was used to measure the intensity of immunofluorescence signal captured by confocal microscopy.

With these techniques four different regions in each tissue section were identified: atrial muscle (AM), transitional area (TA), periphery (SNp) and centre (SNc) of the SN. Summary of data is shown in Fig. 1. The AM is characterised by large densely packed myocytes with little connective tissue and fibroblasts, but high expression of Cx43 and ANP. The TA is characterised by small loosely packed myocytes that contains a mixture of Cx43 and ANP positive and negative cells. The SNp, like TA, also contains a mixture of Cx43 and ANP positive and negative cells, its cells are smaller than AM cells, but similar to TA cells. However, unlike TA cells, SNp cells are embedded in network of connective tissue. The SNc is characterised by much smaller cells embedded in network of connective tissue, contains large number of fibroblasts and little or no Cx43 and ANP. The location and size of the SN, in our study, is in agreement with previous studies (e.g. 4). However, the TA extended further into the AM of the terminal crest and extended beyond the SN towards the ICV. We conclude that the SN is more extensive structure than previously thought, and the large transitional area (which contains a mixture of atrial and nodal cells) could explain the large variation in the position of the leading pacemaker site.

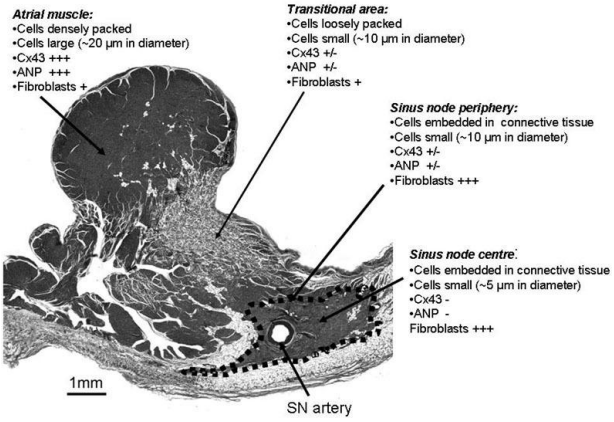

Figure 1. Summary of histology and immunohistochemistry data.

Dobrzynski et al. Circ 111, 846-854.

Fedorov et al. Am J Physiol 291, 612-623.

Boineau et al. Circ 6, 1221-1237.

Sánchez-Quintana et al. Heart 91, 189-194.

Where applicable, the authors confirm that the experiments described here conform with The Physiological Society ethical requirements.

PC19

n-3 and n-6 polyunsaturated fatty acids inhibit the cardiac transient outward K^+ channel, Kv1.4, by slowing recovery from inactivation

N.E. Farag[1], J. Warwicker[1], T.W. Claydon[2] and M.R. Boyett[1]

[1]Human and endocrine sciences, University of Manchester, Manchester, UK and [2]University of British Columbia, Vancouver, BC, Canada

Many studies have shown that polyunsaturated fatty acids from marine sources can prevent ischemia-induced cardiac arrhythmias in animals and probably humans. Kv1.4 is one of the K^+

channels responsible for I_{to} and we have studied the mechanism underlying the effect of arachidonic acid (C20:4n-6; AA), eicosapentaenoic acid (C20:5n-3; EPA) and docosahexaenoic acid (C22:6n-3; DHA) on Kv1.4. The Kv1.4 channel was expressed in *Xenopus* oocytes and currents were recorded using the two-electrode voltage clamp technique. Wild-type Kv1.4 current was inhibited during repetitive pulsing (0.5 Hz) by AA, EPA and DHA as a result of a slowing of recovery from inactivation. For example, 100 μM AA decreased current by 82±0.5 % as a result of a decrease in the time constant of recovery from 2.25±0.14 to 4.12±0.04 s (n=5). In the wild-type channel, whereas N-type inactivation is responsible for inactivation, C-type inactivation controls recovery from inactivation. To study the effect on C-type inactivation directly, we expressed a mutant channel, which lacks N-type inactivation (fKv1.4 Δ2-146). In the mutant channel, AA, EPA and DHA dramatically enhanced the onset of C-type inactivation with a K_D of 43, 15 and 18 μM, respectively. Acidosis enhances C-type inactivation of Kv1.4, while raised extracellular K^+ reduces it. We observed an interaction among the effects of AA, DHA, pH and K^+ on Kv1.4: although 30 μM AA or DHA markedly enhanced C-type inactivation of Kv1.4 when extracellular pH was 7.4 and extracellular K^+ was 3 mM, they had no effect when the pH was reduced to 5.5 or K^+ was raised to 100 mM (n=5). Replacement of either of two positively-charged extracellular residues with a cysteine residue (H508C, K532C) abolishes the effect of extracellular pH and K^+. The same mutations abolished the effect of polyunsaturated fatty acids. Analysis of a comparative model for the structure of the Kv1.4 channel indicates that AA could insert into the membrane just outside of the pore domain. In such a configuration, the negatively-charged headgroup of AA would interact with H508, stabilising it in the protonated state. This effect would in turn influence the selectivity filter and K^+ ion binding, enhancing C-type inactivation. Our model is consistent with the experimental data, since the effect of AA is lost in the H508C mutant. It is concluded that application of polyunsaturated fatty acids, via the positively charged residues, H508 and K532, in the extracellular mouth of the channel, enhance C-type inactivation - this causes a slowing of recovery from inactivation and, thus, an inhibition of current during repetitive pulsing.

Where applicable, the authors confirm that the experiments described here conform with The Physiological Society ethical requirements.

PC20

Reduction of human atrial ITO by chronic beta-blockade is not due to changes in ion channel expression

G.E. Marshall[1], J.O. Tellez[2], J.A. Russell[1], S. Currie[3], M.R. Boyett[2], A.C. Rankin[1], K.A. Kane[3] and A.J. Workman[1]

[1]Cardiovascular Medicine, University of Glasgow, Glasgow, UK, [2]University of Manchester, Manchester, UK and [3]University of Strathclyde, Glasgow, UK

The chronic treatment of patients with a beta-blocker is associated with a prolongation of the atrial cell action potential duration[1]. The transient outward K^+ current (ITO) density is reduced in these patients but there is no change in the voltage or time dependent properties of this current[2]. The mechanisms underlying this reduction in ITO density are unknown.

To test the hypothesis that the expression of atrial ITO channel pore-forming and accessory subunits differs between patients treated or not treated with a beta-blocker.

Right atrial appendage tissue was obtained from 36 consenting patients, in sinus rhythm, undergoing cardiac surgery. Of these patients, 16 were taking beta1-selective blockers for at least 4 weeks prior to surgery. Tissue mRNA and protein levels were measured using real time RT-PCR and western blotting, respectively. Chronic beta-blockade did not change the ratio of the level of mRNA encoding the ITO pore forming protein, Kv4.3, relative to 28S rRNA and GAPDH mRNA [1.8±0.1 vs 1.9±0.2, in beta-blocked (n=8) and non beta-blocked patients (n=8), respectively; mean±s.e.m. Student's t-test, $p>0.05$]. Kv4.3 protein was detected in human atrial tissue at 65 kDa using a monoclonal anti-Kv4.3 antibody (Neuromab). Chronic beta-blockade did not change the ratio of the level of Kv4.3 protein relative to GAPDH [1.2±0.1 vs 1.3±0.3, in beta-blocked (n=8) and non beta-blocked patients (n=10), respectively; $p>0.05$). The relative levels of mRNA encoding various ITO channel accessory proteins that associate with Kv4.3 were unchanged in beta-blocked (n=8) compared to non beta-blocked (n=8) patients: KChIP2 (2.5±0.3 vs 2.7±0.6); KChAP (2.5±v0.1 vs 2.4±0.2); Kvβ1 (3.8±0.2 vs 3.2±0.4); Kvβ2 (1.9±0.1 vs 1.7±0.3) and frequenin (2.0±0.2 vs 1.9±0.3); $p>0.05$ for each.

The reduction in atrial ITO density associated with the chronic treatment of patients with a beta-blocker cannot be explained by changes in the expression of the ion channel pore-forming subunit or by changes in the expression of its regulatory accessory subunit genes.

Workman AJ et al. (2003). Cardiovasc Res 58, 518-525.

Marshall G et al. (2006). Eur Heart J 27, 30 Suppl. (Abstract).

Supported by the British Heart Foundation.

Where applicable, the authors confirm that the experiments described here conform with The Physiological Society ethical requirements.

PC21

Crosstalk between IP_3 and cAMP may mediate the actions of α_1-adrenoceptor agonists in guinea-pig atrial myocytes

T. Collins and D.A. Terrar

Pharmacology, University of Oxford, Oxford, UK

The role of IP_3 in the heart is currently unclear, though reports have suggested a role for IP_3 in atrial muscle through a variety of mechanisms (Lipp et al. 2000 Wang et al. 2005). An important possibility yet to be considered is the involvement of Ca^{2+} stimulated adenylyl cyclases (AC 1 and 8), which have an important role in the sino-atrial node (SAN), particularly AC 1 (Mattick et al. 2007). The aim of this study was to investigate whether IP_3 and cAMP may mediate the effects of phenylephrine on guinea-pig atrial myocyte Ca^{2+} transients.

Male guinea-pigs (300-400 g) were killed by cervical dislocation following stunning. Atrial myocytes were isolated using collagenase, loaded with indo-5F-AM (as the Ca^{2+} probe) and field

stimulated (3ms pulse width, 1Hz; 36°C) to fire action potentials. Data are presented as mean±S.E.M. and P<0.05 (paired Student's t-tests) was taken to indicate statistical significance.
Immunocytochemistry revealed that the type 2 IP_3 receptor (IP_3R) is located sub-sarcolemmally while AC1 and AC8 are associated with the sarcolemma (n>6).
Phenylephrine (10 μM) increased atrial myocyte Ca^{2+} transients by 35±9% (% change in fluorescence ratio for emission at 410 and 490 nm; P<0.01, n=8). This effect was prevented by pretreatment with prazosin (1μM, n=6), an α_1-adrenoceptor antagonist. The effects of phenylephrine were also prevented by 2-APB (2.5μM, n=5), a cell-permeant inhibitor of IP_3Rs, suggesting that IP_3 mediates the response to phenylephrine.
The possibility of constitutive production of cAMP in atrial myocytes, as has been shown in SAN myocytes (Mattick et al. 2007), was also investigated. MDL (10μM), an AC inhibitor, reduced Ca^{2+} transient amplitude by 48±8% (P<0.001, n=7). H89 (1μM), a protein kinase A inhibitor, reduced Ca^{2+} transient amplitude by 37±5% (P<0.001, n=6). IBMX (100μM), a phosphodiesterase inhibitor, increased Ca^{2+} transient amplitude by 85±11% (P<0.001, n=6). These data support the suggestion of constitutive cAMP production.
In the presence of MDL, phenylephrine produced a 12±4% (P<0.05, n=5) increase in Ca^{2+} transient amplitude. This increase was smaller than phenylephrine alone (unpaired Student's t-test, P<0.05).
These data are consistent with phenylephrine stimulating the production of IP_3 which then acts to release Ca^{2+} from the SR. This sub-sarcolemmal Ca^{2+} stimulates the activity of sarcolemmal AC1 and perhaps AC8 to enhance cAMP synthesis, thereby activating protein kinase A to phosphorylate proteins involved in the increase in Ca^{2+} transient amplitude.

Lipp, P., Laine, M., Tovey, SC., Burrell, KM., Berridge, MJ., Bootman, MD. (2000). Current Biology 10, 939-942.

Mattick, PA., Parrington, J., Odia, E., Simpson, A., Collins, T., Terrar, DA. (2007). J Physiol (in press).

Wang, YG., Dedkova, EN., Ji, X., Blatter, LA., Lipsius, SL. (2005). J Physiol 567, 143-157.

This work was supported by the BHF. Thank you to Professor Mikoshiba for the monoclonal IP_3 receptor antibodies.

Where applicable, the authors confirm that the experiments described here conform with The Physiological Society ethical requirements.

PC22

Facilitation of the L-type calcium current in mouse sinoatrial nodal cells

Y. Wu[1] and M.E. Anderson[1,2]

[1]Internal Medicine, Carver College of Medicine, University of Iowa, Iowa City, IA, USA and [2]Physiology, Carver College of Medicine, University of Iowa, Iowa City, IA, USA

L-type Ca2+ current (I(Ca,L)) facilitation is a dynamic pattern of increased peak current and slowed inactivation evoked by repetitive stimulation after rest or increasing frequency of stimulation. Facilitation of I(Ca,L) is an important mechanism for afterdepolarizations in ventricular myocytes and may also contribute to post-rest potentiation. I(Ca,L) also contributes to the generation and modulation of the pacemaker action potential in sinoatrial nodal (SAN) cells. However, the presence and the potential role of I(Ca,L) facilitation in SAN cells is less clear. We measured I(Ca,L) in regularly-beating SAN cells isolated enzymatically from wild-type mice using the whole-cell patch-clamp technique. I(Ca,L) was confirmed by its sensitivity to Nifedipine 5 μM and Isoproterenol 100 nM. The train of the test depolarizations evoked at 0 or 10 mV from a holding potential of -80 mV was applied at 0.5 Hz after at least 3 minutes rest at -80 mV. I(Ca,L) was recorded with Na+ and K+ free (TEA+ substitute for Na+) bath solution and 10 mM EGTA with 3 or 0 mM Ca2+ in the pipette solution. There were no significant changes in SAN cell I(Ca,L) amplitude or inactivation kinetics during a train of repetitive stimuli with 10 mM EGTA and 0 mM Ca2+ in the pipette solution (estimated [Ca2+]i 0.15 pM assuming 10 nM Ca2+ contamination in Millipore water). The average maximal increase in the time integral of I(Ca,L) was 5±2%, and 2±3% in the peak amplitude of I(Ca,L) (n=10). In contrast, I(Ca,L) was dramatically facilitated in ventricular myocytes tested under the same experimental conditions (74±16% increase in the time integral of I(Ca,L) and 18±3% increase in the peak amplitude of I(Ca,L) (n=7)). However, I(Ca,L) facilitation (21±8% increase in integrated I(Ca,L) and 18±5% increase in the peak amplitude of I(Ca,L), n=12) was observed in SAN cells when 3 mM Ca2+ was added to the pipette solution (estimated [Ca2+]i 62 nM). I(Ca,L) facilitation in ventricular myocytes was 94±7% increase in integrated I(Ca,L) and 26±2% increase in the peak I(Ca,L) (n=9) with 3 mM Ca2+ under the same experimental conditions. Facilitation in SAN cells was abolished by pretreatment with ryanodine 10 μM (-3±4% in integrated I(Ca,L) and 1±2% in peak amplitude of I(Ca,L), n=5). Facilitation is also abolished by ryanodine in ventricular myocytes (Wu et al. (2001)). These results show that I(Ca,L) facilitation in mouse SAN cells is less robust and occurs in a narrower window of [Ca2+]i compared to ventricular myocytes. These findings suggest that the dominant L-type calcium channel (CaV1.3) in SAN cells might have a different mechanism of facilitation compared to ventricular myocytes.

Wu Y et al. (2001) J Physiol 535, 679-687

Where applicable, the authors confirm that the experiments described here conform with The Physiological Society ethical requirements.

PC23

Intracellular Ca^{2+} transient modulates cAMP in sinoatrial nodal cells

M.M. van Borren[1], N. Hajji[2], J.G. Zegers[1], A.O. Verkerk[1], H.L. Tan[3], S.L. Peters[2], A.E. Alewijnse[2], E.E. Verheijck[1] and J.H. Ravesloot[1]

[1]Physiology, AMC UvA, Amsterdam, Netherlands, [2]Pharmacology and Pharmacotherapy, AMC UvA, Amsterdam, Netherlands and [3]Experimental Cardiology, AMC UvA, Amsterdam, Netherlands

During the last decade, intracellular calcium (Ca^{2+}_i) transients have been recognized as an important pacemaker mechanism in sinoatrial nodal (SAN) cells. The so called "Ca^{2+}_i clock" directly

depolarizes the membrane potential through activation of the sodium calcium exchange current (I_{NCX})[1]. Recent evidence suggests that Ca^{2+}_i also indirectly increases the funny current (I_f) through activation of Ca^{2+}_i–stimulated adenylyl cyclases (AC1 and AC8)[2,3]. In this study we investigated to what extent acetylcholine (ACh) change Ca^{2+}_i transients and how these changes affect cAMP and pacemaker frequency.

Ca^{2+}_i transients were recorded from isolated rabbit SAN cells using Indo-1 fluorescence. Intracellular cAMP was measured in SAN cells using a LANCE® cAMP 384 Kit and a Victor plate reader.

ACh slowed pacemaker frequency (n=13), decreased cAMP (n=15), inhibited all phases of the Ca^{2+}_i transient (n=13) and reduced the SR Ca^{2+} content (n=7) in a concentration dependent fashion. On the other hand, noradrenaline (NA) speeded pacemaker frequency (n=22), increased cAMP (n=15) and augmented all phases of the Ca^{2+}_i transient (n=22) and increased the SR Ca^{2+} content (n=7). The ACh-mediated changes persisted in the presence of NA, albeit all significantly attenuated.

Inhibition of Ca^{2+}_i transients by 3 μmol/L ryanodine lowered the basal intracellular cAMP concentration (n=7) and intrinsic pacemaker frequency (n=8). Moreover, ryanodine prevented the NA-mediated increase in cAMP (n=7) and pacemaker frequency (n=10). Furthermore, ryanodine facilitated the ACh-mediated inhibition of cAMP (n=7) and pacemaker frequency slowing (n=10) in the presence of NA. Similar cAMP changes were obtained when Ca^{2+}_i was buffered with 25 μmol/L BAPTA-AM (n=3).

Here we show that ACh decreases Ca^{2+}_i transients, cAMP levels, and pacemaker frequency. In addition, all effects of ACh were attenuated by NA-stimulation. Finally, Ca^{2+}_i transients control cAMP production and pacemaker frequency. The latter observation provides an indirect mechanism by which Ca^{2+}_i can modulate cAMP-dependent currents, such as I_f, and pacemaker frequency.

Bogdanov KY, Maltsev VA, Vinogradova TM, Lyashkov AE, Spurgeon HA, Stern MD, Lakatta EG (2006). Circ Res 99, 979-987.

Bucchi A, Baruscotti M, Robinson RB, DiFrancesco D (2003). J Mol Cell Cardiol 35, 905-913.

Mattick PA, Parrington J, Odia E, Simpson A, Collins T, Terrar DA (2007). J Physiol (in press).

This work was supported by a grant from the Dutch Organization for Scientific Research (ALW 805-06-153) and the Dutch Heart Association (NHS 96.039).

Where applicable, the authors confirm that the experiments described here conform with The Physiological Society ethical requirements.

PC24

A computer model of the interaction between N-type and C-type inactivation in Kv1.4 channels

G.C. Bett[1,2], I.D. Madou[2], V.E. Bondarenko[2] and R.L. Rasmusson[2]

[1]Gynecology-Obstetrics, University at Buffalo, SUNY, Buffalo, NY, USA, [2]Physiology and Biophysics, University at Buffalo, SUNY, Buffalo, NY, USA and [3]University at Buffalo, SUNY, Buffalo, NY, USA

Kv1.4 channels are voltage-gated potassium channels which produce a rapidly inactivating current, which is thought to be the molecular basis of the transient outward current seen in the endocardium of several mammalian species. Kv1.4 channels exhibit two distinct inactivation mechanisms. Fast "N-type" inactivation is well characterized, and operates by a "ball and chain" mechanism. The slower C-type inactivation is not so well defined, but involves conformational changes of the pore resulting in a block of current. We studied the interaction between these inactivation mechanisms using two electrode voltage clamp of Kv1.4 and Kv1.4ΔN (amino acids 2-146 deleted from the N-terminal to prevent N-type inactivation) cloned channels heterologously expressed in Xenopus oocytes. We manipulated C-type inactivation by altering extracellular potassium concentration and introducing a point mutation that diminishes C-type inactivation.

We developed a computer model of Kv1.4ΔN (C-type inactivation) and Kv1.4 (N- and C-type inactivation) channels to determine the required degree of interaction between the inactivation mechanisms needed to replicate the experimental data. Using our four closed state model with distinct N- and C-type inactivated states, it was not possible to reproduce the experimental data without allowing direct transitions between the N- and C-type inactivated states. We examined this model in conjunction with a model of permeation and binding to potassium in the pore. The permeation model reproduces the conductance activity relationship of Kv1.4. In the context of inactivation/channel block, movement of potassium from the intracellular side of the channel to the outside cannot change occupancy of the external site when physiological levels of extracellular potassium are present. Changes in occupancy of the pore contribute only a small fixed energy in the presence of extracellular potassium.

C-type inactivation is the rate-limiting step which determines recovery from inactivation, so understanding C-type inactivation, and how it is coupled to N-type inactivation is critical in understanding how a channel will act to repetitive stimulation in vivo. Our study suggests that N-type inactivation and, by similarity, open pore drug binding, interact with C-type inactivation primarily through an allosteric mechanism.

Where applicable, the authors confirm that the experiments described here conform with The Physiological Society ethical requirements.

PC25

A computer model of molecular heterogeneity in the mouse heart

V.E. Bondarenko and R.L. Rasmusson

Physiology and Biophysics, University at Buffalo, SUNY, Buffalo, NY, USA

In many mammalian cardiac tissues, molecular heterogeneity of repolarizing currents produces significant spatial heterogeneity and/or dispersion of repolarization. However, the ability of the mouse heart to sustain physiologically relevant heterogeneity of repolarization has recently been questioned, based on the small size of the murine heart.

We used our previously published comprehensive computer model of the mouse action potential (Bondarenko *et al.* 2004) to predict the ability of mouse cardiac tissue to maintain spatial

gradients of repolarization due to differential expression of membrane channels. Our model tissue consisted of two cell types (apex and septum) arranged as either a linear fiber (cable) or a ring. Adjacent myocytes were connected by gap junctions. The approximate circumference of the mouse heart surface is ~19 mm. Our tissue model was therefore constructed of 190 cells, which, given an average cell length of ~100 μm, approximates the dimensions of the mouse heart.

Our simulations of action potential (AP) propagation in multicellular rings or cables predict that substantial gradients in repolarization and intracellular $[Ca^{2+}]_i$ transients can be maintained through heterogeneity of expression of K^+ channels over a distance of about ten cells. This gradient can cause transient block of propagation. Simulation of AP propagation in inhomogeneous (with an abrupt inhomogeneity between apical and septal cells) and uniform (apex) cables stimulated from the apex with pacing period $\tau = 69$ ms showed block at the boundary of the two cell phenotypes due to differential repolarization at high stimulation rates. This block was caused by a transient increase in AP duration in the septum region of the tissue model, which was the result of inactivation of slowly recovering K^+ currents. In contrast, the AP in the uniform apical tissue showed only periodic behavior. In addition, the abruptness of gradients of ion channel expression as well as the site of stimulation were capable of causing $[Ca^{2+}]_i$ transient oscillations and affected the stability of $[Ca^{2+}]_i$ dynamics. Alternans occurred as a result of a complex interaction between the ionic and electrotonic currents and the Ca^{2+} fluxes in the cell, when exposed to repeated rapid stimulation. The major impact of this growing complexity is on the gating behavior of the ryanodine sensitive Ca^{2+} release mechanism in the sarcoplasmic reticulum. When abrupt channel expression gradients were introduced, alternans was observed at slower pacing rates than when gradual changes were used.

Our simulations demonstrate that microscopic aspects of tissue organization are important for predicting large scale propagation phenomena and that the mouse heart should be able to sustain substantial molecularly based heterogeneity of repolarization.

Bondarenko *et al.* (2004). *Am J Physiol Heart Circ Physiol* **287**, H1378-403.

Where applicable, the authors confirm that the experiments described here conform with The Physiological Society ethical requirements.

PC26

The effect of different fixatives on immunodetection of ion channels in isolated rat ventricular cells

T.T. Yamanushi[1], E. Hirakawa[1], H. Ohsaki[1], M.R. Boyett[2] and H. Dobrzynski[2]

[1]Kagawa Prefectural College of Health Sciences, Takamatsu City, Japan and [2]Division of Cardiovascular and Endocrine Sciences, University of Manchester, Manchester, UK

Immunocytochemistry with a standard formaldehyde fixation can pose difficulty in regard to sub-cellular localisation of ion channel proteins in cardiac cells. The aim of this study was to compare the effect of different fixatives on the expression and sub-cellular localisation of various ion channels in isolated ventricular cells from rats. Animals were killed humanely and cells isolated. Fixative used were: (1) aldehyde fixative (10% buffered formalin, FA); (2) non-aldehyde fixatives (a. 100 % methanol, MeOH, b. 100 % acetone and c. absolute ethanol, EtOH); (3) combination of fixatives (1) and (2a).

After treatment with various fixatives, ventricular cells underwent a standard immunocytochemical protocol. In brief, cells were incubated with primary IgGs (raised against ion channel proteins listed in Table 1), and then incubated with secondary IgGs conjugated to either FITC or Cy3. Immunofluorescence signal was visualised with confocal microscopy.

It is clear from Table 1., that the strength of immunofluorescnce signal of various channel proteins and their sub-cellular immunolocalisation in isolated ventricular myocytes varies amongst different fixation protocols. For example, a stronger intensity of immunolabelling of $K_v1.5$, $K_v4.2$, $Ca_v1.2$, $Ca_v1.3$ and $Ca_v\alpha1$, was detected with the non-aldehyde fixative such MeOH (2a) than that with the aldehyde fixative (1). Conversely, immunofluorescence signals for $K_{ir}6.2$, $Na_v1.1$ and $Na_v1.5$ were better detected with either the aldehyde fixative (1) or combination of fixatives (1) and (2a) than that non-aldehyde fixative (e.g., 2a). In addition, the sub-cellular localisation of ion channel proteins varied between the aldehyde fixative (1) and the non-aldehyde fixative (2a). With former fixative there was no immunosignal of e.g., $K_v1.5$ and $K_v4.2$ at the intercalated discs. Our data suggest that MeOH is the most suitable non-aldehyde fixative for the detection of ion channel proteins by immunocytochemistry.

Table 1. Summary of data

Ion channel	FA	MeOH	MeOH-FA	FA-MeOH	Acetone	EtOH
$K_v1.5$ ($I_{K,ur}$)	+/- T	+/- T + ID	+/- T + ID	+/- T + ID	+/- T + ID	+ ID
$K_v4.2$ (I_{to})	-	+ T + ID	-	+ ID	n/a	n/a
$K_{ir}6.2$ ($I_{K,ATP}$)	+/- T +/- N	+/- N	+/- T +/- N	+/- T	n/a	n/a
$Na_v1.1$ (I_{Na})	+ T +/- ID, +/- N + S	+/- T + S	+/- T +/- ID, +/- N + S	+/- T + ID	+/- T +/- S	+/- S
$Na_v1.5$ (I_{Na})	+/- T +/- ID + S	+/- T +/- ID +/- S	-	+ ID + S	-	+/- S
$Ca_v1.2$ ($I_{Ca,L}$)	-	+ T +/- N	-	+ T + ID	n/a	n/a
$Ca_v1.3$ ($I_{Ca,L}$)	+/- T	+ T	-	-	n/a	n/a
$Ca_v\alpha1$ ($I_{Ca,L}$)	+/- T	+ T + ID	-	-	n/a	n/a

T, t-tubules; ID, intercalated disks; N, nucleus; S, sarcolemma; n/a, not examined. Signal for each ion channel was collected from n=3 or more cells.

Supported by BHF, British Council and Daiwa Foundation.

Where applicable, the authors confirm that the experiments described here conform with The Physiological Society ethical requirements.

PC27

Prediction of the electrical activity of the human atrioventricular node using a quantitative PCR-based approach

I.D. Greener[1], N.J. Chandler[1], J.O. Tellez[1], P. Molenaar[2], D.C. Sigg[3], V. Sharma[3], M.R. Boyett[1] and H. Dobrzynski[1]

[1]Cardiovascular and Endocrine Sciences, University of Manchester, Manchester, UK, [2]University of Queensland, Queensland, QLD, Australia and [3]Medtronic Inc., Minneapolis, MN, USA

The complex electrophysiological behaviour of the mammalian atrioventricular node (AVN) compared to other regions of the heart is well known. Numerous clinical investigations have

described various electrophysiological phenomena unique to the human AVN. However, little is known about the molecular nature of ionic currents responsible for this electrical activity.

The aim of our study was to use quantitative PCR (QPCR) to identify ion and gap junction channels and membrane protein subunits governing the electrical activity in the human AVN. Three AVN samples (with surrounding working myocardium) were cryosectioned and specific sub-regions: compact node (CN), His bundle (HB), atrial muscle (AM) and ventricular muscle (VM)] were microdissected. Total RNA was extracted from these regions and cDNA synthesised, and used for QPCR analysis (ABI 7900HT). Hearts were obtained from the Queensland Heart Valve Bank.

The ion channel transcripts in Table 1 were analysed for the level of abundance across different tissue types, and amongst each group of transcripts within each tissue type. For example, when compared to different tissue types, Cx43 was the least abundant in the CN. However, when compared to different connexins within the CN, Cx40 was the most abundant. Interestingly, out of all transcripts investigated, the Ca^{2+} handling proteins showed the most abundant mRNA levels in the working myocardium as well as the AVN, whereas amongst the ion channels (after HERG), the twin-pore K^+ (TWIK1), together with HCN4, appear to be the second most abundant ion channel subunits in the human AVN.

We have shown that the two sub-regions of the human AVN to contain a unique ion channel expression profile compared to working myocardium. Our data provide insights into the electrical function of the AVN.

Table 1. Summary of expression profile of ion channel and gap junction channel, and Ca^{2+} handling protein subunits throughout cardiac tissues.

Ion channel group	Ion channel subunit	Compact node	His bundle	Atrial muscle	Ventricular muscle
Pacemaker channels	HCN1 HCN2 HCN3 HCN4	+ +++ - ++++	+ + - ++	++ + - +	++ ++ - +
Na^+ channel	Nav1.5 Nav1.3 Nav1.6 Nav1.7 Navβ1 Navβ2 Navβ3 Navβ4	++ - - - +++ - - -	+++ - - - ++ - - -	+++ - - - ++++ - - -	+++++ + - - +++++ - - +
Ca^{2+} channels	Cav1.3 Cav1.2 Cav3.1 Cav3.3	++ +++ + -	+ ++ - -	- +++ - -	- ++++ - +
K^+ channels	Kv1.4 Kv1.5 Kv4.2 Kv4.3 KvB1 KvB2 FREQ KvLQT1 KCNJ2 HERG	+ +++ + ++ - + +++ + + + +++++	+ - + + - + ++ + + ++++	+ + + ++ - +++ + + ++ +++	++ - - +++ + ++ ++ + ++++ ++++++
Connexins	Cx31.9 Cx40 Cx43 Cx45	- ++++ ++ ++	- +++ +++ +	- ++ ++++ +	- + ++++ +++
Ca^{2+} handling proteins	NCX1 RYR2 RYR3 SERCA2a	+ + - ++	+ ++ - +	++ +++ - +++	+++ +++++ - ++++
Other	TWIK1 MIRP2 MIRP3 β1 adrenergic receptor β2 adrenergic receptor	++++ - - +++ +++	++ - - + ++	+++ - - +++ +++	++ - - +++ ++++

Where applicable, the authors confirm that the experiments described here conform with The Physiological Society ethical requirements.

PC28

Effects of 4-aminopyridine and temperature on the spontaneous electrical activity of sinoatrial area of the murine heart

D.A. Lavrik and V.A. Golovko

Institute of Physiology, Komi Science Centre, Urals Branch, Russian Academy of Sciences, Syktyvkar, Russian Federation

4-aminopyridine (4-AP)-sensitive current, ITO, participates in the generation of action potentials (AP) in the right atrium cells of the murine heart; however, its functional role is unclear. The aim of our study was to investigate the influence of 4-aminopyridine (4-AP) on main AP parameters of cells in sinoatrial (SA) area of the murine heart. We also analyzed the localization of the pacemaker cells in the right atrium and the dependence of AP parameters on the temperature.

Experiments were carried out on the spontaneously beating right atrial strips isolated from hearts of 2-month-old male albino mice (n=10), using the standard microelectrode technique. Data are shown mean± SD.

The mouse sinoatrial node is located parallel to the crista terminalis and is separated from the surrounding atrial muscle by an atrial septum. Very little is known about the main parameters of AP in SA area of the murine heart. The SA area has heterogeneous electrophysiological characteristics; therefore, we have divided all registered AP into four types: 1. Dominant pacemaker; 2. Latent pacemaker; 3. Atrial-like AP without phase 1 and without slow diastolic depolarization; 4. Atrial-like AP with phase 1 and without slow diastolic depolarization.

The mean frequency of AP generation was 201±18 and varied from 55 to 280 min-1 under control conditions (K+ 5.4 mM, Ca2+ 1.8 mM, 31 °C). The decrease in the perfusion solution temperature from 32 to 24 °C was accompanied by an increase in the duration of the AP at 20% and 90% of repolarization (APD20, APD90) and in the cycle length (CL), according to the exponential dependence (r2 = 0, 88±0,4). The values of Q10 coefficient for APD20, APD90 and CL were 2.5–3.0 at the 32–23 °C temperature range. The cessation of AP generation by the pacemaker cells was registered at the temperature 17±0.5 °C.

The supplementation of the perfusion solution with 4-AP (1.6 mM, "Sigma") led to decrease in the AP amplitude and an increase of the following parameters: APD20 in 3 times, APD50 – 2 times, APD90 – 1.5 times, and CL – nearly 4 times, as compared to the control. Seven minutes after the 4-AP exposure, the AP generation in the atrial-like cells with phase 1 was blocked, and their contractions were completely discontinued. This effect was reversible by 5-minute reperfusion.

Additionally, we found that the AP amplitude was greater in the latent pacemaker cells than in the true pacemaker cells. 4-aminopiridine (1.6 mM) blocked the AP generation in the atrial cells and the contraction activity of the sinoatrial area strips.

Where applicable, the authors confirm that the experiments described here conform with The Physiological Society ethical requirements.

PC29

Mathematical model of the atrioventricular node

S. Inada[1], J.C. Hancox[2], H. Zhang[1] and M.R. Boyett[1]

[1]University of Manchester, Manchester, UK and [2]University of Bristol, Bristol, UK

Mathematical models can be a repository of knowledge as well as important research and teaching tools. Although models of the action potential have been developed for most regions of the heart, there is no biophysically-detailed model for the atrioven-

tricular node (AVN) and the aim of this study was to develop such a model. We have developed models of the action potential in single atrio-nodal (AN), nodal (N), and nodal-His (NH) cells of the rabbit AVN based on published electrophysiological data. Using these single cell models, together with single cell models of the sinoatrial node (SAN) (Zhang et al. 2000) and atrial muscle (AM) (Lindblad et al. 1996), we have developed a simplified one-dimensional (1D) model including the SAN and AVN (Fig. 1A). This model consisted of a string of 50 SAN cells (central and peripheral SAN cells) connected to a string of 150 atrial cells. The atrial cells are connected to two parallel pathways, a slow pathway (SP) (a string of 50 atrial cells and 150 N cells) and a fast pathway (a string of 50 atrial cells and 150 AN cells). Both pathways are connected to a string of 50 NH cells. Neighbouring cells are coupled by a coupling conductance. The single cell models have the same action potential characteristics (maximum diastolic potential, upstroke velocity, amplitude, and action potential duration) and refractoriness as observed in experiments (Fig. 1B). Using the 1D model, we simulated action potential propagation. Under normal conditions, action potentials were initiated in the centre of the SAN and then propagated through the atrium and AVN (Fig. 1C). Using the 1D model excluding the SAN, we analysed the characteristics of the AV node. After stimulation of the atrial muscle, the action potential propagated along the parallel slow and fast pathways, but conduction along the fast pathway was faster than conduction along the slow pathway. After premature stimulation, conduction along the fast pathway was blocked, and then AVN reentry could occur. After slow pathway ablation or partial block of the L-type Ca2+ current, AVN reentry was abolished. During atrial fibrillation, the AV node limited the number of action potentials transmitted to the ventricle. Pacemaker activity arose from the slow pathway in the absence of SAN pacemaking. These results are consistent with experimental data. In conclusion, we have developed the first biophysically-detailed model of the AVN and it shows many of the typical physiological and pathophysiological characteristics of the tissue. The model can be used as a tool to analyse the complex structure and behaviour of the AV node.

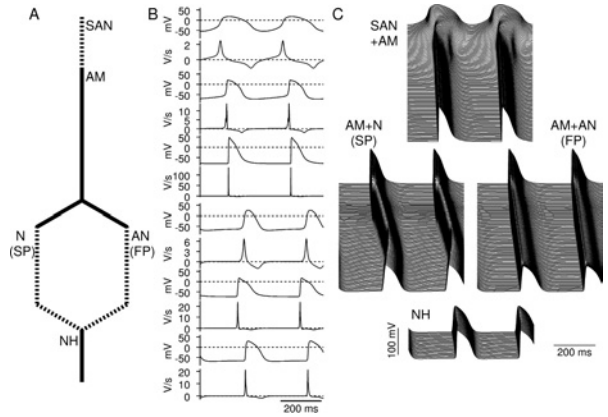

Fig. 1. Simulated action potentials in 1D model from SAN to AVN

Lindblad D et al. (1996). *Am J Physiol* **271**, H1666-H1696.

Zhang H et al. (2000). *Am J Physiol* **279**, H397-H421.

Where applicable, the authors confirm that the experiments described here conform with The Physiological Society ethical requirements.

PC30

Dynamic action potential clamp as a tool for comparing ionic mechanisms in cardiac cell models

A.P. Benson, A.S. Rhodes and A.V. Holden

Institute of Membrane and Systems Biology, University of Leeds, Leeds, UK

In the dynamic action potential (AP) clamp, the membrane potential is forced to follow that of a real or modelled AP and membrane currents are measured (1). We apply the technique to different computational models describing cardiac cell electrophysiology to evaluate the relative roles of ionic current components in models with different AP shapes. This process is illustrated by identifying the ionic mechanisms for the different effects of rapid and slow delayed rectifier current (I_{Kr} and I_{Ks}) block on the formation of early afterdepolarisations (EADs) in human and guinea pig ventricular midmyocardial cell models.

EADs can occur in the Luo-Rudy dynamic (LRd) guinea pig model (2) with 40% block of I_{Kr} or 70% block of I_{Ks} (3), but in the Ten Tusscher and Panfilov (TP) human model (4) 93% block of both I_{Kr} and I_{Ks} is required for EAD formation (5). This could simply be due to the different AP shapes, or may be a consequence of differing contributions of different currents to AP repolarisation and/or to different reactivation kinetics of the L-type Ca^{2+} current $I_{Ca,L}$ that is responsible for EAD development. We therefore used the dynamic AP clamp technique to impose the same waveforms (either LRd guinea pig or TP human solitary APs) on each of the two models. During both guinea pig and human AP clamps, the repolarising currents I_{Kr} and I_{Ks}, the Na^+-Ca^{2+} exchanger current I_{NaCa}, and the inward rectifier current I_{K1}, had the same relative contributions to the total repolarising current in both models. However, the inactivation gates of $I_{Ca,L}$ recovered from inactivation more slowly in the TP human model, compared to the LRd guinea pig model. Regardless of waveform, the $I_{Ca,L}$ voltage-dependent inactivation gate f had recovered to $f \approx 0.86$ in the LRd model at time of 90% AP repolarisation, but to only $f \approx 0.46$ in the TP model. The f gate recovers to $f = 0.4$ at approximately 84% and 95% of AP duration in the LRd and TP models respectively (again, regardless of waveform). Therefore, a relatively longer prolongation of the AP is required in the TP human model (313 ms or 75%, compared to 77 ms or 35% in LRd) for sufficient reactivation of $I_{Ca,L}$ and subsequent EAD formation to occur.

We conclude that the reduced propensity for EAD formation in the TP human model, compared to the LRd guinea pig model, is due primarily to the slower kinetics of $I_{Ca,L}$ recovery from inactivation, and that a greater block of I_{Kr} and I_{Ks} is required only to sufficiently prolong the AP. We propose that the dynamic AP clamp can be utilised to compare other aspects of normal and pathological electrophysiology between different cardiac cell models.

Wilders R (2006). *J. Physiol.* **576**, 349-359.

Luo CH & Rudy Y (1994). *Circ. Res.* **74**, 1071-1089.

Viswanathan PC & Rudy Y (1999). *Cardiovasc. Res.* **42**, 530-542.

Ten Tusscher KHWJ & Panfilov AV (2006). *Am. J. Physiol.* **291**, H1088-H1100.

Benson AP *et al.* (2007). *Chaos* **17**, 015105.

APB is supported by the Dr Hadwen Trust for Humane Research.

Where applicable, the authors confirm that the experiments described here conform with The Physiological Society ethical requirements.

PC31

Propagation of the action potential through a 3D model of the rabbit right atrium including the conduction system

J. Li[1], J.E. Schneider[2], I.D. Green[1], H. Dobrzynski[1] and M.R. Boyett[1]

[1]University of Manchester, Manchester, UK and [2]University of Oxford, Oxford, UK

Accurate simulation of the generation and propagation of cardiac electrical activity requires detailed electrophysiological and anatomical models. We have previously generated three-dimensional (3D) anatomical models of the sinoatrial node and the atrioventricular node (Dobrzynski et al., 2005; Li et al, 2004). The purpose of this study was to construct a 3D anatomical model of the rabbit right atrium with multiple objects, including the conduction system, and use this to simulate the propagation of the action potential through the right atrium. In this work, we used multiple techniques to generate the 3D anatomical model. The model was based on ~1500 images of the rabbit heart (atria and part of ventricles) obtained by high-resolution magnetic resonance imaging (MRI). MATLAB was used to analyse the data and generate a 3D anatomical model of the right atrium. The ~1500 two-dimensional images were stacked to produce a 3D array. Segmentation was carried out semi-manually by analysing the data using custom written programs developed in MATLAB. The sinoatrial node (SAN) and atrioventricular node (AVN) could be detected (and then segmented) after comparison of images with our existing models of the SAN and AVN. A 3D right atrium array model, including thirteen objects, was constructed. The objects are the right atrium, the SAN, the AVN, part of the right ventricle, the aorta with the aortic valve, the superior vena cava, the inferior vena cava, the coronary sinus, the tricuspid valve, part of the mitral valve, the fossa ovalis, the central fibrous body and outer fatty and connective tissue. The FitzHugh-Nagumo model was used to simulate the propagation of the action potential from the SAN through the 3D right atrium model. The propagation sequence is shown in Fig. 1.

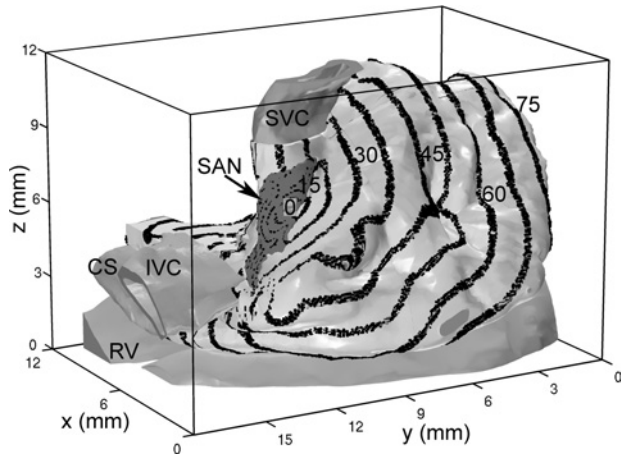

Figure 1. The propagation sequence of the action potential through the 3D right atrium. Isochrones are shown at 7.5 ms intervals.

Dobrzynski H et al. (2005). Circulation 111, 846-854.

Li J et al. (2004). Computers in Cardiology 31, 89-92.

Where applicable, the authors confirm that the experiments described here conform with The Physiological Society ethical requirements.

PC32

The role of transient outward potassium current in mammalian heart

L. Virag[1], A. Kristof[3], P.P. Kovacs[1], Z. Horvath[3], Z. Nagy[1], C. Lengyel[2], N. Jost[3], J.G. Papp[1,3] and A. Varro[1,3]

[1]Department of Pharmacology and Pharmacotherapy, University of Szeged, Szeged, Hungary, [2]1st Department of Internal Medicine, University of Szeged, Szeged, Hungary and [3]Division of Cardiovascular Pharmacology, Hungarian Academy of Sciences, Szeged, Hungary

Previous studies suggested that transient outward potassium current (Ito) plays an important role only during the early fast phase of repolarization, modulating the plateau phase potential, but its direct influence on the total repolarization is negligible. In this study we took advantage of the observation that at high (100 μM) concentration chromanol 293B blocks not only the slow delayed rectifier (IKs), but also largely inhibits Ito. Therefore, in the presence of full IKs block (by L-735,821) chromanol 293B induced change of action potential (AP) and of ionic currents can be attributed to its effect on Ito. Based on this assumption, the aim of the present study was to investigate the role of Ito in cardiac ventricular repolarization applying the standard microelectrode and patch-clamp techniques.

Chromanol 293B (100 μM), in the presence of full IKs block (100nM L-735,821), lengthened the AP repolarization in both endocardial and epicardial dog right ventricular preparations. The next set of experiments was carried out in the presence of 100 nM dofetilide and 1 μM BayK 8644 to impair the repolarization reserve of the preparations. In these measurements chromanol 293B excessively lengthened the AP compared to that found after application of another IKs inhibitor, HMR-1556, which can be attributed to the Ito blocking effect of chromanol 293B. In single dog ventricular myocytes the inactivation kinetics of Ito current was biexponential (rapid phase: 3.89±0.13 ms, amplitude: 2222±239 pA; slow phase: 23.5±2.5 ms, amplitude: 172±33 pA; n=12, test potential: 20 mV, means±S.E.M.). The amplitude and the time constant of the slow phase of Ito imply an important role of the slowly inactivating Ito in the plateau phase of the action potential. The little overlap of the inactivation and activation curves over the potential range of 0 to –40 mV proposes that a small fraction of these ion channels may reactivate in this potential range (Ito "window current"). The Ito current during the AP plateau and repolarization phases was measured as chromanol 293B sensitive current in left ventricular myocytes isolated from dog hearts using an AP waveform for the command potential. It was found that Ito carries significant outward current in the plateau and also in the later phase of repolarization of the AP.

We concluded that the transient outward potassium current may influence not only indirectly, by modulating the plateau potential, but also directly the ventricular repolarization in the heart.

Gima K & Rudy Y (2002). Circ Res 90, 889-896.

Sun X & Wang HS (2005). J Physiol 564.2, 411-419.

Supported by OTKA NI-61902, ETT T-542/2006 grants and Bolyai Research Scholarship (NJ and CL).

Where applicable, the authors confirm that the experiments described here conform with The Physiological Society ethical requirements.

PC33

Mechanism of Ca intracellular alternans produced by low depolarization - A study by a stochastic Ca handling model

T. Tao[1], S.C. O'Neill[2], S. Kharche[1] and H. Zhang[1]

[1]Biological Physics Group, School of Physics and Astronomy, The University of Manchester, Manchester, UK and [2]Unit of Cardiac Physiology, School of Medicine,, The University of Manchester, Manchester, UK

Mechanical alternans in cardiac muscle is believed to be associated with intracellular Ca alternans. Mechanisms underlying intracellular Ca alternans are unclear. In previous experimental study we produced alternans of systolic Ca under voltage clamp by applying small depolarizing pulses. The aim of this study is to investigate by computer modeling how such alternans of systolic Ca is produced.

A mathematical model of coupled cluster of 60 Ca release units is developed. Each release unit contains a stochastic unitary L-type Ca channel modeled by 12 states of Markovian chain model developed by Jafri et al, a subspace, a cytoplasm space and sarcoplasmic reticulum (SR) release channel and uptake sites (SERCA). Inter-units coupling is via Ca diffusion between neighbouring cytoplasm spaces and from subspaces to cytoplasm spaces. A series of voltage stimulus pulses, which steps from a -40 mV to -20 mV, was used to simulate low depolarization as we used in our previous experimental study. The model was paced by 1 Hz. During stimulation, at each Ca unit, localized Ca transient ([Ca]i) at cytoplasmic space and SR content were recorded and plotted in the time-space format.

The 12-state Markovian chain model can reproduce the channel current of a single unitary L-type channel, and a minimal of upto 5000 channels are required to reproduce the properties of L-type Ca channel I-V relationship as seen at whole cell level. Corresponding to a series of small depolarization pulses, systolic Ca alternans were observed, during which a large Ca transient was followed by a small Ca transient. The simulated Ca alternans was consistent with our experimental observations, being generated by propagating waves of Ca release and sustained through an alternation of SR Ca content.

This study provides novel and fundamental insights to understand how the low pulse affects the behavior of unitary L-type channel and the mechanisms underlying intracellular Ca alternans produced by low depolarization.

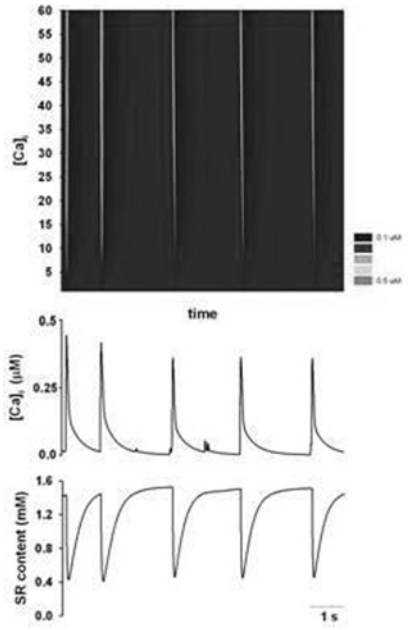

Diaz ME, O'Neill SC, & Eisner DA (2004). Circ Res 94, 650-656.

Jafri MS, Rice JJ, Winslow RL (1998). Biophys J 74, 1149-1168.

Y Kurata, I Hisatome, S Imanishi and T Shibamoto (2002). Am J Physiol Heart Circ Physiol 283, H2074-H2101.

Supported by BBSRC and BHF.

Where applicable, the authors confirm that the experiments described here conform with The Physiological Society ethical requirements.

PC34

Pacemaker activity and ionic channels in mouse atrioventricular node cells

L. Marger[1], J. Striessnig[2], J. Nargeot[1] and M.E. Mangoni[1]

[1]Physiology, Institute of Functional Genomics, CNRS UMR5203, Montpellier, Hérault, France and [2]Abteilung Pharmakologie und Toxikologie, Institut fur Pharmazie und Centrum fur Molekulare Biowissenschaften, Innsbruck, Austria

Pacemaker activity of the sino-atrial node (SAN) initiates the heartbeat under normal conditions. The atrio-ventricular node (AVN) also displays pacemaker activity and can take over the control the heartbeat upon SAN failure. The molecular bases of AVN automaticity are poorly understood. We have isolated spontaneously beating cells from the mouse AVN region and studied ionic channels and pacemaker activity by employing the whole-cell configuration of the patch-clamp technique. Upon enzymatic isolation, 10% of cells displayed spindle-shaped morphology and regular beating. Spontaneously-active AVN cells displayed intrinsic slower pacing rate compared to SAN cells (180± 15 bpm in n=11 AVN cells vs. 280± 20 bpm in n=7 SAN cells, $p<0.05$). The maximum pacing rate measured upon stimulation by 100 nM isoproterenol was higher in SAN than in AVN cells (350±10 bpm, vs 240± 20 bpm, $p<0.01$). The hyperpolarization-activated current, (If) was found in all SAN and AVN cells tested. If density and that of the inward rectifier current

(IK1) were respectively lower and higher in AVN (If density:17± 4 pA/pF in AVN and 39± 4 pA/pF in SAN, n=10 p<0.05) that in SAN cells. In three AVN cells tested, If inhibition by 3μM zeneca inhibited pacing by 30%, indicating an important role for this current in AVN automaticity. The density of the L-type Ca2+ current (ICa,L) was lower in AVN than in SAN cells (1.7±0.2 n=6, vs 4.8±0.3, n=5, p<0.05). AVN cells lacking L-type Cav1.3 Ca2+ channels (from Cav1.3-/ mice) had strongly reduced pacemaker activity. Indeed, upon 10 cells investigated, only 4 Cav1.3-/- AVN cells displayed pacemaker activity. Both cardiac-TTX resistant and TTX-sensitive Na+ currents were found in AVN cells. Blocking TTX-sensitive currents by 100 nM TTX significantly reduced pacemaker activity (from 260± 16 bpm to 221± 18 bpm n=8, p<0.05), leaving unaffected the action potential (AP) waveform, while blocking both TTX-sensitive and TTX-resistant channels with 20 μM TTX strongly reduced pacemaking (from 210± 22 bpm to 80 ± 22 bpm, n=8, p<0.01) and affected the AP upstroke and duration. Delayed-rectifier (IKr) current was consistently found in automatic AVN cells. In contrast, no KvLQT1 related (IKs) or transient outward (Ito) current were found. We conclude that both If and Cav3.1 channels play an important role in automaticity of AVN cells. Enhanced expression of IK1 in AVN cells, together with reduced expression of If, ICa,L can in part explain the intrinsic faster pacing in the SAN cells compared to AVN.

Supported by the French National Association for Research (ANR). L. Marger acknowledges a PhD student fellowship from the GRRC.

Where applicable, the authors confirm that the experiments described here conform with The Physiological Society ethical requirements.

PC35

Gender differences in ion channel gene expression in the sinus node and right atrium

J.O. Tellez, J. Yanni, H. Musa, M.R. Boyett and H. Dobrzynski

University of Manchester, Manchester, UK

The functional properties of the sinus node (SN) and atrium are known to differ with gender: as compared to women, men have a lower extrinsic and intrinsic heart rate1 and a 1.5 fold higher chance of developing atrial fibrillation[2] (AF). To investigate the gender differences, we used quantitative PCR (qPCR) to compare ion channel gene expression in the SN and right atrium (RA) from young adult male (n=6) and female (n=6) Wistar Hannover rats. qPCR was carried out using an ABI 7900HT instrument with ABI Taqman probe assays to measure the relative abundance of 96 transcripts. In the SN, expression of the L-type Ca^{2+} channel $Ca_v1.3$ was 76% lower in the male ($P < 0.05$). In the RA, there were significant ($P< 0.05$) gender differences in 20% of the transcripts investigated, including $Ca_v\alpha2\delta3$ and $Ca_v\beta2$ (accessory subunits for the L-type Ca^{2+} channel), $K_v1.2$ (contributes to I_{to}), $K_v1.5$ (responsible for $I_{K,ur}$) and K_vLQT1 (responsible for $I_{K,s}$). All differences between the male and female RA corresponded to lower expression in the male. There were more significant differences between the SN and RA in the male (51% of transcripts), than in the female (15% of transcripts). For example, in the male but not the female, $Na_v1.1$ (contributes to I_{Na}), $Ca_v3.1$ (contributes to $I_{Ca,T}$) and $K_v1.5$ were significantly more abundant in the SN, whereas Kir2.1(contributes to $I_{K,1}$) was significantly less abundant in the SN. $Ca_v1.3$ plays an important role in pacemaking in the SN, and a lower expression of this channel could possibly explain the lower intrinsic heart rate of the male. In AF, there is a reduction in the L-type Ca^{2+} current[3], I_{to} and $I_{K,ur}$. Could a lower expression of $Ca_v\alpha2\delta3$, $Ca_v\beta2$, $K_v1.2$ and $K_v1.5$ in the male RA contribute to the higher incidence of AF in men? The higher expression of K_vLQT1 in the female RA is surprising as gain of function mutations in K_vLQT1 have been linked with AF. The mRNA abundance for the intracellular Ca^{2+} handling proteins SERCA2a, NCX1 and IP3 Receptor Type I expression were significantly less abundant in the male RA. This again could have important implications for the function of the RA of the different genders. In addition, $Ca_v1.3$ and $K_v1.5$ protein was detected by western blotting, in both male and female SN and RA. In summary, our data show potentially important gender differences in ion channel expression in the SN and RA. The gender differences in ion channel gene expression in the RA could aid in understanding the mechanisms responsible for AF.

Bazett H. (1920). *Heart.* 7, 353-370.

Feinberg WH et al. (1995). *Arch Intern Med.* 155, 469-473.

Van Wagoner DR et al. (1999). *Circ Res.* 85, 428-436.

Where applicable, the authors confirm that the experiments described here conform with The Physiological Society ethical requirements.

PC36

Adenovirus-mediated transgene expression in the sinus node and development of a bradycardic model for the *in vitro* study of biopacemaking in sick sinus syndrome

G.M. Morris[1], M.R. Boyett[1], P.A. Kingston[2], M. Lei[1] and H. Dobrzynski[1]

[1]Cardiac Electrophysiology, University of Manchester, Manchester, UK and [2]Vascular Gene Therapy Unit, University of Manchester, Manchester, UK

Diseases of the sinus node (SAN) are common leading to bradycardia requiring electronic pacemaker implantation.[1] To avoid problems associated with such devices efforts have been made to develop biological pacemakers by ion channel expression in the myocardium.[2] Our aim is to apply this concept to the diseased SAN. Wistar rats were killed humanely, the SAN was dissected as previously described.[3] Control (n=4) and 'sick sinus' preparations (inferior portion after division below level of leading pacemaker site; n=4) were then cultured. Electrical activity was monitored using 0.15 mm stainless steel electrodes. Tissue was frozen and sections prepared, Masson's trichrome and immunostaining (caveolin 3) were performed as previously described.[4] The sick sinus model displayed a slower rate than the control, and both slowed over a five day period (170 ± 12.5 to 124 ± 10.8 beats per minute (bpm) and 277 ± 9.7 to 211 ± 13.4 bpm respectively [mean ± SEM]). No histological changes were seen with Masson's trichrome staining (n=3) and there was no change in cell size as assessed with Caveolin3 immunostaining (n=10). Further preparations (n=2) were injected with 1×10^8 infectious units of adenovirus Ad5-PREP-lacZ and expression of β-galactosidase was assessed by X-gal staining after 48 h. Tissue sections were prepared and immunostaining (ANP and

HCN4) performed as above. X-gal staining of whole SAN infected with Ad5-PREP-lacZ showed transgene expression at injection sites in the superior and mid SAN. 15 μm X-gal stained sections revealed high levels of lacZ expression in the SAN area. Immunostaining for ANP (negative marker for SAN), and HCN4 (positive marker for SAN) confirmed transgene expression was in the SAN (figure 1). This method provides a useful in vitro model of pathological bradycardia and furthermore the tissue is receptive to adenovirus infection with high levels of transgene expression in the SAN. This provides proof of concept for the use of this model to study sinus node biopacemaking as a potential treatment for sick sinus syndrome.

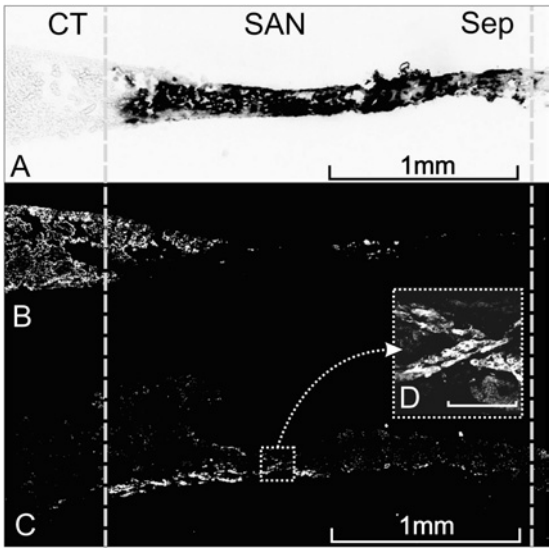

Figure 1. Adjacent sections prepared from rat SAN following injection with $1x10^8$ infectious units of Ad5-PREP-lacZ with tissue culture for 48 h. A, β-galactosidase expression assessed by X-gal staining (dark area) (CT, crista terminalis; Sep, interatrial septum). B, C, immunolabelling for ANP (B) and HCN4 (C). D, high power image of immunolabelling for HCN4 in the area indicated by the dotted box. The white areas in b, c and d represent positive labelling; scale bar in box d is 100 μm.

Gregoratos G et al (2002). J Cardiovasc Electrophysiol 13, 1183-1199.

Rosen MR (2007). Heart 93, 145-146.

Dobrzynski H et al (2000). J Histochem Cytochem 48, 769-780.

Dobrzynski H et al (2005). Circulation 111, 846-854.

Where applicable, the authors confirm that the experiments described here conform with The Physiological Society ethical requirements.

PC37

Post-natal developmental changes in Ca^{2+} handling proteins in rabbit sinoatrial node and atrium

E.S. H Abd Allah, J.O. Tellez, M.R. Boyett and H. Dobrzynski

Cardiovascular Research Group, University of Manchester, Manchester, UK

The sinoatrial node (SAN) has spontaneous activity and sets the heart rate. The intrinsic heart rate (heart rate in absence of autonomic agonists) is faster in the neonate as compared to the adult. Intracellular Ca^{2+} plays an important role in the spontaneous activity. Ca^{2+} is released from the sarcoplasmic reticulum (SR) through the RYR2 Ca^{2+} release channel into the cytosol; it is then removed either into the SR via the SR Ca^{2+} pump (SERCA2a) or out of the cell via the Na^+-Ca^{2+} exchanger (NCX1). Removal of Ca^{2+} via NCX1 produces an inward current, which contributes to the initiation of a spontaneous action potential in the SAN. Ca^{2+} reenters the cell via the Ca^{2+} channels, $Ca_v1.2$ and $Ca_v1.3$. The aim of this study was to investigate Ca^{2+} handling proteins in the SAN and right atrium (RA) during post-natal development. 11 neonatal (2-7 days of age) and 11 adult male (~6 months of age) New Zealand white rabbits were killed humanly and the expression of Ca^{2+} handling proteins at the mRNA level was measured using quantitative PCR (qPCR) and the distribution of Ca^{2+} handling proteins was measured using immunohistochemistry. Cx43 (major gap junction channel in heart) was used as a negative marker of the SAN, and caveolin3 (membrane bound protein) was used as a marker of myocytes and was a useful tool to measure cell diameter. Tables 1 and 2 summarise the qPCR and immunohistochemistry data. Our data show that during development there is a complex change in the expression and distribution of Ca^{2+} handling proteins. Interestingly, using caveolin3, our data also show that there is a significant increase in cell diameter in the SAN and atrial muscle with age. We conclude that there are complex developmental changes in Ca^{2+} handling proteins in the SAN, as well as in the RA, and these changes may, in part, explain the observed decrease in the intrinsic heart rate from the neonate to the adult. The results also may have implications for excitation-contraction coupling in the atrial muscle.

Table 1. Summary of qPCR data.

mRNA	neonate RA vs. adult RA	neonate SAN vs. adult SAN	neonate RA vs. neonate SAN	adult RA vs. adult SAN
SERCA2a	< (P<0.05)	=	> (P<0.05)	> (P<0.001)
RYR2	< (P<0.05)	=	=	> (P<0.01)
NCX1	=	> (P<0.05)	< (P<0.05)	=
Cav1.2	=	=	=	=
Cav1.3	=	> (P<0.05)	< (P<0.001)	< (P<0.05)
Cx43	< (P<0.05)	=	> (P<0.001)	> (P<0.05)

Table 2. Summary of immunohistochemical data.

Protein	Adult RA	Neonate RA	Adult SAN	Neonate SAN
SERCA2a	close to sarcolemma & diffuse near nucleus	diffuse near nucleus	diffuse near nucleus	diffuse near nucleus
RYR2	close to sarcolemma & internal striation	close to sarcolemma	close to sarcolemma	close to sarcolemma
NCX1	sarcolemma	sarcolemma	sarcolemma	sarcolemma
Cx43	intercalated discs	intercalated discs	absent	absent

Where applicable, the authors confirm that the experiments described here conform with The Physiological Society ethical requirements.

PC38

Modelling conduction through the Purkinje-ventricular junction and the short-QT syndrome associated with HERG mutation in canine ventricles

O.V. Aslanidi[1], P. Stewart[1], M.R. Boyett[2] and H. Zhang[1]

[1]School of Physics & Astronomy, The University of Manchester, Manchester, UK and [2]School of Medicine, The University of Manchester, Manchester, UK

Excitation conducted through the Purkinje fibres (PF) to the ventricles determines synchronized timing and sequencing of ventricular contraction. However, marked differences in action

potential (AP) morphology and duration between the PF and ventricular cells may lead to abnormalities in excitation conduction through the Purkinje-ventricular junction (PVJ). The aim of this study is to develop a novel electrophysiologically detailed model for the canine PF cell, and link it to the existing 3D computer model of the canine ventricular wedge in order to explore excitation conduction through the PVJ into the ventricles under physiological and pathological conditions. The 3D wedge model has been developed earlier [1] to incorporate detailed geometry and fibre orientation of the canine left ventricular free wall and transmural AP heterogeneity between epicardial (epi), midmyocardial (M) and endocardial (endo) ventricular cells. The canine endo cell AP model [1] was modified to incorporate detailed voltage-clamp experimental data on characteristics of all major ion channels in the canine PF cells [2]. The model was validated by its ability to reproduce AP restitution properties similar to various experimental measurements for the canine PF cells. Finally, the single Purkinje cell model was incorporated into a fibre entering the 3D ventricular wedge model, with intercellular electrical coupling conductances chosen to produce AP propagation velocities of about 1.5 m/s and 0.5 m/s for the PF and the ventricular tissues, respectively [3]. Simulations of the resultant model produced physiologically realistic transmural action potential duration (APD) dispersion patterns, as well as a conduction time delay of about 5 ms at the PVJ reported in experiments [3]. The removal of voltage-dependent inactivation of the delayed rectified current, I_{Kr}, was used to simulate pathological short QT syndrome (SQTS) associated with a gain-in-function of I_{Kr} channel due to HERG N588K mutation [4]. Such "mutant" I_{Kr} resulted in heterogeneous APD shortening among epi, M, endo and PF cells, which augmented the transmural APD dispersion at the PVJ and shortened the QT interval in pseudo-ECG by about 70 ms. This provides causative link between HERG N588K mutation to SQTS. In summary, the constructed detailed 3D model provides a powerful computational tool for non-invasive studies of electrical phenomena within and around the heterogeneous PVJ. Shortening of the QT interval under the defected I_{Kr} inactivation conditions substantiates a link between SQTS and the HERG N588K mutation.

Benson AP *et al.* (2007) *Prog Biophys Mol Biol*, in press.

Han W *et al.* (2001) *Circulation* **104**: 2095-2100.

Wiedmann RT *et al.* (1996) *Am J Physiol* **271**: 1507-16.

Zhang H *et al.* (2004) *Biochem Biophys Res Comm* **322**: 693-99.

This research was supported by the BBSRC.

Where applicable, the authors confirm that the experiments described here conform with The Physiological Society ethical requirements.

PC39

Modulation of heart rate in the simple planktonic crustacean *Daphnia* by temperature and by caffeine concentration

A. Elliott and N. Pinnington

Faculty of Life Sciences, University of Manchester, Manchester, UK

Although many crustaceans have their pacemaking centre outside the heart in a cardiac ganglion, some very simple crustaceans are reported to have myogenic hearts. One such is the primitive planktonic freshwater crustacean *Daphnia*, whose single-chambered heart can beat over a wide range of frequencies. In evolutionary terms, Daphnids are intermediate between insects (arthropoda, hexapods) and more advanced crustaceans. Here we report changes in Daphnia heart with altered temperature and with application of caffeine.

Intact Daphnia were immobilized within a small chamber of the stage on an inverted microscope and heart wall motion measured using a video edge detector (Crescent Electronics) or by analysis of digital images using ImageJ. Temperature in the chamber was measured with a bead thermistor.

Daphnia heart rate was highly temperature dependent, falling from 320-330 min^{-1} at room temperature (21°C) to around 50 min^{-1} at 3°C. The rate of both contraction and relaxation also decreased dramatically. Filling and ejection fraction increased with reduced temperature. Occasional arrhythmias were seen on rapid cooling to 3-4°C.

The addition of caffeine progressively slowed heart rate, by a maximum of around 20% at 15-20 mM caffeine. Caffeine-treated hearts showed a similar temperature-dependent decrease in heart rate as control hearts, but showed more arrhythmias on cooling. Arrhythmias were most common at 5-7°C in caffeine-treated hearts, and hearts that were not arrhythmic on cooling to 3°C often became transiently arrhythmic as they rewarmed slightly.

The systems responsible for cardiac pacemaking in Daphnia remain unknown. In the tubular heart of Drosophila, recent gene-targeting studies implicate SERCA (Sanyal et al. 2006) and the twin-pore K^+ (K2P) channel dORK1 (Lalevée et al. 2006) in pacemaking. Although Daphnia heart contains SR (Stein et al. 1966), the effects of caffeine reported here suggest the SR is not required for pacemaking. From the recently completed *Daphnia pulex* genome we have identified genes encoding SERCA, RyR, multiple K2P channels homologous to dORK1, and a single HCN channel homologue. Further studies will be required to identify which of these mechanisms regulate cardiac pacemaking in Daphnia.

Lalevée N *et al.* (2006). *Curr Biol* **16**, 1502-1508.

Sanyal S *et al.* (2006). *J Comp Physiol B* **176**, 253-263.

Stein RJ *et al.* (1966). *J Cell Biol* **29**, 168-170.

The sequence data used for this analysis were produced by the US Department of Energy Joint Genome Institute http://www.jgi.doe.gov/

Where applicable, the authors confirm that the experiments described here conform with The Physiological Society ethical requirements.

PC40

Transmural gradient and differential distribution of Nav1.5 in the cardiac conduction system in mouse heart

C. Remme[1], B. Scicluna[1], M.J. van den Hoff[1], A.A. Wilde[1], M.W. Veldkamp[1], T.A. van Veen[2], J.M. de Bakker[1,3] and C.R. Bezzina[1]

[1]Heart Failure Research Center, Academic Medical Center, Amsterdam, Netherlands, [2]Medical Physiology, University Medical Center, Utrecht, Netherlands and [3]Interuniversity Cardiology Institute, Utrecht, Netherlands

Mutations in the SCN5A gene encoding the cardiac sodium channel protein Nav1.5 are associated with multiple arrhythmia syn-

dromes, including Brugada syndrome, long QT3 syndrome, conduction disease, and sinus node dysfunction. Knowledge of cardiac distribution of Nav1.5 is currently limited but may be crucial for understanding the complex mechanisms involved in sodium channelopathies. Therefore, we investigated Nav1.5 protein expression in various components of the conduction system and transmural layers of the ventricular wall in mouse heart tissue sections.

We performed immunohistochemistry and confocal laser scanning microscopy on heart tissue cryosections from adult mice. Nav1.5 showed low to absent expression in the sinoatrial and atrioventricular nodes, whereas the hyperpolarization activated cyclic nucleotide-gated potassium channel 4 (Hcn4) was highly expressed in these areas. In contrast, high expression levels of Nav1.5 were observed in the His bundle and bundle branches (as shown by co-localization with Hcn4). Thus, Hcn4 considered typical for nodal like pacemaker cells and Nav1.5 are not mutually exclusive throughout the entire conduction system. In both ventricles, a transmural gradient was observed, with a low Nav1.5 labeling intensity in the subepicardial layer as compared to midmural; highest Nav1.5 labeling intensity was observed in the subendocardium. The subepicardial layer with low Nav1.5 expression comprised a larger fraction of the total ventricular wall in the right compared to the left ventricle. Overall, the labeling intensity of Nav1.5 within the heart was: His bundle/bundle branches > subendocardium > midmural myocardium >> subepicardium >>> sinoatrial/atrioventricular nodes.

The sodium channel protein Nav1.5 shows heterogeneous distribution within the cardiac conduction system, underlying the diverse conduction disorder phenotypes in sodium channelopathies. Decreased Nav1.5 expression in the subepicardium may render the right ventricle in particular more susceptible to sodium channel dysfunction. Thus, transmural heterogeneity in Nav1.5 protein expression may constitute a novel pathophysiological player involved in Brugada syndrome.

This study was supported by the Netherlands Heart Foundation (Grant 2003/B195).

Where applicable, the authors confirm that the experiments described here conform with The Physiological Society ethical requirements.

PC41

A differential role for f- and Cav1.3-channels in the genesis and regulation of heart rate: physiological effects of I_f inhibition by ivabradine in mice lacking L-type Cav1.3 Ca^{2+} channels

L. Marger[1], M. Bouly[2], H. Aptel[1], A. Leoni[4], A. Cohen-Solhal[1], J. Striessnig[3], F. Mahlberg-Gaudin[2], J. Nargeot[1] and M.E. Mangoni[1]

[1]Physiology, Institute of Functional Genomics, CNRS UMR5203, Montpellier, Hérault, France, [2]Institut de Recherche Internationales Servier (IRIS), Courbevoie, France, [3]Abteilung Pharmakologie und Toxikologie Institut fur Pharmazie und Centrum fur Molekulare Biowissenschaften, Universitat Innsbruck, Innsbruck, Austria and [4]Institut du Thorax, Inserm U533, Nantes, France

The I_f and the Cav1.3-mediated L-type Ca^{2+} currents play important roles in the genesis of cardiac automaticity and heart rate (HR). The differential role of f- and Cav1.3- channels in pacemaking is not completely elucidated. More importantly, it is not known if automaticity can persist after inhibition and/or inactivation of both f- and Cav1.3 channels. The effects of I_f inhibition by ivabradine (IVA), the first specific and selective I_f sinus node inhibitor, were investigated on ECG parameters using telemetry in wild-type (WT; n=7) and Cav1.3 knockout (Cav1.3-/-; n=7) mice, spontaneously bradycardic. IVA was administrated once intra-peritoneally (ip bolus) from 0.1 up to 6 mg/kg. In WT and Cav1.3-/- mice, IVA dose-dependently reduced the mean HR (Fig.) without affecting the QRS complex. At 3 mg/kg, mean HR reduction was –23 and –39% in WT and Cav1.3-/- ($p<0.01$), respectively. Saturation of IVA effect on HR was observed between 3 and 6 mg/kg, suggesting complete and specific in vivo inhibition of I_f at these doses. In Cav1.3-/- mice, intrinsic HR measurement after injection of atropine (0.5 mg/kg ip) and propranolol (1 mg/kg ip) (A+P) to block autonomic input, showed that I_f inhibition by IVA at 3 mg/kg ip did not stop pacemaking but only lowered intrinsic HR from 226±34 bpm at 3 mg/kg to 184±24 bpm with A+P at the same dose ($p<0.05$). In conclusion, f- and Cav1.3 channels control the mean HR. I_f inhibition lowered both the mean and maximal HR. Contrary to f-channels, Cav1.3 channels do not reduce the maximal HR, but stabilize HR. Most importantly, both normal and intrinsic pacemaker activity can persist in the absence of Cav1.3 channels even after partial inhibition of HCN channels. These observations indicate that multiple mechanisms contribute to cardiac automaticity and, thus to the safety of HR reducing agents such as ivabradine.

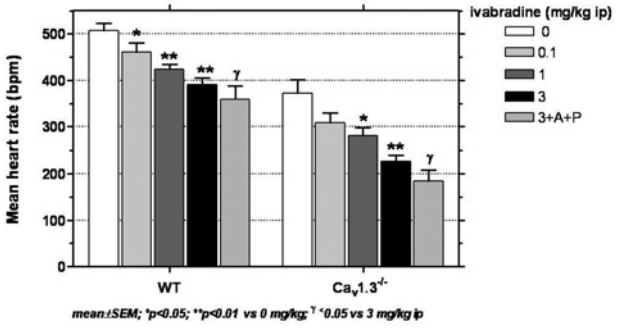

Supported by IRIS and the French National Association for Research (ANR).

Where applicable, the authors confirm that the experiments described here conform with The Physiological Society ethical requirements.

PC42

Diabetes mellitus modifies the electrical activity from rabbit atrioventricular node

A. Albarado Ibáñez[1], R. Berra Romani[2], V. Hernández García[3], J.A. Sanchez-Chapula[4] and J.T. Jacome[2,1]

[1]Physiology, Benemérita Universidad Autónoma Puebla (BUAP), Puebla, Mexico, [2]Facultad de Medicina, BUAP, Puebla, Mexico, [3]ICB, Universidad Autónoma de Ciudad Juárez, Ju√É¬°rez, Mexico and [4]CUIB, Universidad de Colima, Colima, Mexico

TITLE ONLY